

Revisiting the Lie-group symmetry method for turbulent channel flow with wall transpiration

George Khujadze^{1*} & Michael Frewer²

¹ Chair of Fluid Mechanics, Universität Siegen, 57068 Siegen, Germany

² Trübnerstraße 42, 69121 Heidelberg, Germany

November 11, 2018

Abstract

The Lie-group-based symmetry analysis, as first proposed in [Avsarkisov *et al.* \(2014\)](#) and then later modified in [Oberlack *et al.* \(2015\)](#), to generate invariant solutions in order to predict the scaling behavior of a channel flow with uniform wall transpiration, is revisited. By focusing first on the results obtained in [Avsarkisov *et al.* \(2014\)](#), we failed to reproduce two key results: (i) For different transpiration rates at a constant Reynolds number, the mean velocity profiles (in deficit form) do not universally collapse onto a single curve as claimed. (ii) The universally proposed logarithmic scaling law in the center of the channel does not match the direct numerical simulation (DNS) data for the presented parameter values. In fact, no universal scaling behavior in the center of the channel can be detected from their DNS data, as it is misleadingly claimed in [Avsarkisov *et al.* \(2014\)](#). Moreover, we will demonstrate that the assumption of a Reynolds-number *independent* symmetry analysis is not justified for the flow conditions considered therein. Only when including also the viscous terms, an overall consistent symmetry analysis can be provided. This has been attempted in their subsequent study [Oberlack *et al.* \(2015\)](#).

But, also the (viscous) Lie-group-based scaling theory proposed therein is inconsistent, apart from the additional fact that this study of [Oberlack *et al.* \(2015\)](#) is also technically flawed. The reason for this permanent inconsistency is that their symmetry analysis constantly involves several unphysical statistical symmetries that are incompatible to the underlying deterministic description of Navier-Stokes turbulence, in that they violate the classical principle of cause and effect. In particular, as we consequently will show, the matching to the DNS data of the scalar dissipation, being a critical indicator to judge the prediction quality of any theoretically derived scaling law, fails exceedingly.

Keywords: *Symmetries, Lie Groups, Scaling Laws, Symmetry Breaking, Turbulence, Channel Flow, Wall Transpiration, Statistical Mechanics, Higher-Order Moments, Closure Problem, Causality;*

PACS: 47.10.-g, 47.27.-i, 47.85.-g, 05.20.-y, 02.20.-a, 02.50.-r

1. Motivation and objectives

The main purpose of this investigation is first to reveal in how far the work of [Avsarkisov *et al.* \(2014\)](#) can be reproduced. With focus on the results obtained from Lie-group analysis, we will re-examine all derivations and conclusions in [Avsarkisov *et al.* \(2014\)](#). One of the key results obtained therein was that of a new *universal* logarithmic scaling law in the center (core region) of a plane turbulent channel flow with uniform wall-normal transpiration. The derivation of this law, presented in [Avsarkisov *et al.* \(2014\)](#) as [Eq. (3.16)]

$$\bar{U}_1 = A_1 \ln \left(\frac{x_2}{h} + B_1 \right) + C_1, \quad (1.1)$$

where $A_1 = k_{\bar{U}_1}/k_1$, $B_1 = k_{x_2}/(hk_1)$ are two group[†] and C_1 one arbitrary integration constant, is

*Email address for correspondence: george.khujadze@uni-siegen.de

†The constant B_1 as defined in [Avsarkisov *et al.* \(2014\)](#) misses a factor $1/h$ in order to be dimensionally correct.

based on three independent scaling symmetries [Eqs. (3.2)-(3.4)] and two independent translation symmetries [Eqs. (3.5)-(3.6)] of the two-point correlation (TPC) equations [Eqs. (2.12)-(2.16)] for the purely inviscid case $\nu = 0$.[†] The emergence of the particular scaling law (1.1) from these just mentioned symmetries is due to the externally set constant transpiration velocity v_0 , which acts as a symmetry breaking parameter in the scaling of the mean wall-normal velocity \bar{U}_2 through the single constraint $k_1 - k_2 + k_s = 0$ [Eq. (3.15)]. Central to the claim of Avsarkisov *et al.* (2014) is that when matching the new logarithmic law (1.1) to direct numerical simulation (DNS) data, then this law turns out to be a *universal* one when written in its deficit form (normalized to the mean friction velocity u_τ as defined in [Eq. (2.1)][‡])

$$\frac{\bar{U}_1 - C_1}{u_\tau} = \frac{1}{\gamma} \ln \left(\frac{x_2}{h} + B_1 \right), \quad (1.2)$$

where all involved matching parameters γ , B_1 and C_1 are independent of the transpiration rate and Reynolds number. In particular, after a fit to the given data, the following universal values were proposed (Avsarkisov *et al.*, 2014, Sec. 4, pp. 116-119):

$$\gamma = 0.3, \quad B_1 = 0, \quad C_1 = U_B, \quad (1.3)$$

where γ is the new universal scaling coefficient to be distinguished from the usual von Kármán constant κ of the near-wall logarithmic scaling law, and where U_B is the mean bulk velocity [Eq. (2.4)] which was kept universally constant in all performed simulation runs for different transpiration rates and Reynolds numbers (due to a fixed overall mass-flow rate employed in the used DNS code; for more details, see also Avsarkisov (2013)).

Our investigation on all these derived and proposed results involve three independent parts. After introducing the governing statistical equations and admitted Lie symmetries in Section 2 with the information only as given in Avsarkisov *et al.* (2014), we will demonstrate the following:

(i) The DNS-data-matched value of A_1 in (1.1), namely $A_1 = u_\tau/\gamma$, is inconsistent to its theoretically derived value $A_1 = k_{\bar{U}_1}/k_1$ composed of two group constants, which are, by construction, independent of the friction velocity u_τ .

(ii) Fig. 9 (a) and (c) in Avsarkisov *et al.* (2014) cannot be reproduced when using the DNS data made available by the authors on their institutional website [fdy]. Neither does the data universally collapse onto a single curve for different blowing parameters in particular, nor does the logarithmic scaling law (1.2) with the proposed parameters (1.3) directly fit to this data.

(iii) For the inviscid ($\nu = 0$) case, as particularly realized in Avsarkisov *et al.* (2014), as well as for the viscous ($\nu \neq 0$) case, as subsequently modified in Oberlack *et al.* (2015), the Lie-group-based scaling theory shows in both cases a methodological inconsistency in that certain higher order velocity correlation functions cannot be matched anymore to the DNS data, despite involving all *a priori* known symmetries of the underlying statistical transport equations. The simple reason for this inconsistency is that several participating symmetries are unphysical in violating the classical principle of cause and effect.

[†]Note that the large-Reynolds-number asymptotics in the cited reference Oberlack (2000) was performed differently than as claimed in the beginning of Sec. 3.1 on p. 109 in Avsarkisov *et al.* (2014). Not for $|\mathbf{r}| \leq \eta$, but rather, oppositely, only for $|\mathbf{r}| \geq \eta$ it was shown that all viscous terms in the TPC equations vanish. For a corresponding English explanation of the ‘‘asymptotic analysis’’ performed in Oberlack (2000), see e.g. Oberlack (2002); Oberlack & Guenther (2003) or Khujadze & Oberlack (2004). Hence, oppositely as claimed, the symmetry analysis in Avsarkisov *et al.* (2014) was *not* performed on equations which have undergone a prior singular asymptotic analysis in the sense $\nu \rightarrow 0$, but instead, only on equations which just result from considering the purely inviscid (Euler) case $\nu = 0$.

[‡]In Appendix A we repeat the basic derivation of relation [Eq. (2.1)] in Avsarkisov *et al.* (2014) to acknowledge this result more carefully.

2. Governing statistical equations and admitted symmetries

Since the aim in Avsarkisov *et al.* (2014) is to investigate within the inviscid ($\nu = 0$) TPC equations [Eqs. (2.12)-(2.15)] only large-scale quantities, such as the mean velocity or the Reynolds stresses, we will proceed accordingly by considering these TPC equations already in their one-point limit ($\mathbf{x}^{(2)} \rightarrow \mathbf{x}^{(1)} = \mathbf{x}$, or in relative coordinates as $\mathbf{r} = \mathbf{x}^{(2)} - \mathbf{x}^{(1)} \rightarrow \mathbf{0}$):[†]

$$\frac{\partial \bar{U}_k}{\partial x_k} = 0, \quad (2.1)$$

$$\frac{\partial \bar{U}_i}{\partial t} + \bar{U}_k \frac{\partial \bar{U}_i}{\partial x_k} + \frac{\partial \bar{P}}{\partial x_i} + \frac{\partial \tau_{ik}}{\partial x_k} = 0, \quad (2.2)$$

$$\frac{\partial \tau_{ij}}{\partial t} + \bar{U}_k \frac{\partial \tau_{ij}}{\partial x_k} + \frac{\partial \tau_{ijk}}{\partial x_k} + \tau_{ik} \frac{\partial \bar{U}_j}{\partial x_k} + \tau_{jk} \frac{\partial \bar{U}_i}{\partial x_k} + \frac{\partial p}{\partial x_i} u_j + u_i \frac{\partial p}{\partial x_j} = 0, \quad (2.3)$$

where

$$\tau_{ij} = \overline{u_i u_j}, \quad \tau_{ijk} = \overline{u_i u_j u_k}, \quad (2.4)$$

are the Reynolds stresses and the third-order (one-point) velocity moments, respectively. Note that in this one-point limit all higher-order continuity constraints [Eqs. (2.14)-(2.15)] either collapsed into the single constraint (2.1) or turned into trivial zero identities.

Referring to the cited study Oberlack & Rosteck (2010) in Avsarkisov *et al.* (2014), it has been shown that a simple and systematic structure for all symmetries is revealed if for the infinite hierarchy of multi-point correlation (MPC) equations the instantaneous (full) field approach is used (instead of the fluctuating, the so-called Reynolds-decomposed field approach as given above). In the one-point limit the corresponding full-field representation of the inviscid TPC equations reads:

$$\frac{\partial \bar{U}_k}{\partial x_k} = 0, \quad (2.5)$$

$$\frac{\partial \bar{U}_i}{\partial t} + \frac{\partial \bar{U}_i \bar{U}_k}{\partial x_k} + \frac{\partial \bar{P}}{\partial x_i} = 0, \quad (2.6)$$

$$\begin{aligned} \frac{\partial \bar{U}_i \bar{U}_j}{\partial t} + \frac{\partial \bar{U}_i \bar{U}_k}{\partial x_k} \bar{U}_j + \bar{U}_i \frac{\partial \bar{U}_j \bar{U}_k}{\partial x_k} + \frac{\partial \bar{P}}{\partial x_i} \bar{U}_j + \bar{U}_i \frac{\partial \bar{P}}{\partial x_j} &= 0, \\ &= \frac{\partial}{\partial x_k} \overline{U_i U_j U_k} \end{aligned} \quad (2.7)$$

which, of course, turns exactly into the system (2.1)-(2.3) when decomposing the full fields into their mean and fluctuating part, i.e., by performing a usual Reynolds field decomposition[‡]

$$U_i = \bar{U}_i + u_i, \quad P = \bar{P} + p. \quad (2.8)$$

Although both representations (2.1)-(2.3) and (2.5)-(2.7) are equivalent, the latter one has the unreckoned advantage, according to Oberlack & Rosteck (2010), of being a linear system which makes the extraction of Lie symmetries considerably easier.

For the specific flow considered in Avsarkisov *et al.* (2014), both systems (2.1)-(2.3) and (2.5)-(2.7) equivalently reduce further. Considered is a statistically stationary plane channel flow of width $w = 2h$ with a mean constant wall-normal transpiration $\bar{U}_2 = v_0$. In the streamwise direction the flow is driven by constant mean pressure gradient, which we will denote as K , in particular $\partial \bar{P} / \partial x_1 = -K$, where $K > 0$ is some arbitrary but fixed positive value. Finally, due

[†]Similar to the strategy as proposed, e.g., in Oberlack & Guenther (2003) [pp. 462-466] or Khujadze & Oberlack (2004) [pp. 395-399], only large scale quantities as the mean velocity and Reynolds stresses are investigated via the inviscid ($\nu = 0$) TPC equations including their one-point limit. For small scale quantities as the dissipation, the viscous TPC equations are needed, which (in their one-point limit) will be discussed later in Section 5.2.

[‡]Note that in order to obtain the explicit form of equation (2.3) from (2.7), the decomposed equation (2.6) has to be used as an auxiliary equation.

to spanwise homogeneity and a spanwise reflection symmetry in this flow, the mean spanwise velocity as well as all velocity moments involving an uneven number of spanwise velocity fields vanish. Hence, for the just-stated assumptions, the full-field system (2.5)-(2.7) reduces to:[†]

$$\frac{\partial \bar{U}_2}{\partial x_2} = 0, \quad (2.9)$$

$$\frac{\partial \bar{U}_1 \bar{U}_2}{\partial x_2} + \frac{\partial \bar{P}}{\partial x_1} = 0, \quad \frac{\partial \bar{U}_2 \bar{U}_2}{\partial x_2} + \frac{\partial \bar{P}}{\partial x_2} = 0, \quad \bar{U}_1 \bar{U}_3 = \bar{U}_2 \bar{U}_3 = 0, \quad (2.10)$$

$$\frac{\partial \bar{U}_1 \bar{U}_2 \bar{U}_2}{\partial x_2} + \frac{\partial \bar{P}}{\partial x_1} \bar{U}_2 + \bar{U}_1 \frac{\partial \bar{P}}{\partial x_2} = 0, \quad \frac{\partial \bar{U}_i \bar{U}_j \bar{U}_2}{\partial x_2} + \frac{\partial \bar{P}}{\partial x_i} \bar{U}_j + \bar{U}_i \frac{\partial \bar{P}}{\partial x_j} = 0, \text{ for } i = j, \quad (2.11)$$

while its corresponding Reynolds decomposed system (2.1)-(2.3) equivalently reduces to:

$$\frac{\partial \bar{U}_2}{\partial x_2} = 0, \quad (2.12)$$

$$\bar{U}_2 \frac{\partial \bar{U}_1}{\partial x_2} + \frac{\partial \bar{P}}{\partial x_1} + \frac{\partial \tau_{12}}{\partial x_2} = 0, \quad \underbrace{\bar{U}_2 \frac{\partial \bar{U}_2}{\partial x_2}}_{=0} + \frac{\partial \bar{P}}{\partial x_2} + \frac{\partial \tau_{22}}{\partial x_2} = 0, \quad \tau_{13} = \tau_{23} = 0, \quad (2.13)$$

$$\left. \begin{aligned} \bar{U}_2 \frac{\partial \tau_{12}}{\partial x_2} + \frac{\partial \tau_{122}}{\partial x_2} + \underbrace{\tau_{12} \frac{\partial \bar{U}_2}{\partial x_2}}_{=0} + \tau_{22} \frac{\partial \bar{U}_1}{\partial x_2} + \frac{\partial p}{\partial x_1} \bar{u}_2 + \bar{u}_1 \frac{\partial p}{\partial x_2} = 0, \\ \bar{U}_2 \frac{\partial \tau_{ij}}{\partial x_2} + \frac{\partial \tau_{ij2}}{\partial x_2} + \tau_{i2} \frac{\partial \bar{U}_j}{\partial x_2} + \tau_{j2} \frac{\partial \bar{U}_i}{\partial x_2} + \frac{\partial p}{\partial x_i} \bar{u}_j + \bar{u}_i \frac{\partial p}{\partial x_j} = 0, \text{ for } i = j. \end{aligned} \right\} \quad (2.14)$$

When considering the list of TPC symmetries [Eqs. (3.2)-(3.6)] as analyzed in Avsarkisov *et al.* (2014), then the reduced Reynolds-decomposed system (2.12)-(2.14) admits the symmetries[‡]

$$\begin{aligned} \bar{T}_1 : \quad x_i^* &= e^{k_1} x_i, \quad \bar{U}_i^* = e^{k_1} \bar{U}_i, \quad \bar{P}^* = e^{2k_1} \bar{P}, \quad \tau_{ij}^* = e^{2k_1} \tau_{ij}, \\ \tau_{ijk}^* &= e^{3k_1} \tau_{ijk}, \quad \overline{\frac{\partial p}{\partial x_j}}^* = e^{2k_1} \overline{\frac{\partial p}{\partial x_j}}, \end{aligned} \quad (2.15)$$

$$\begin{aligned} \bar{T}_2 : \quad x_i^* &= x_i, \quad \bar{U}_i^* = e^{-k_2} \bar{U}_i, \quad \bar{P}^* = e^{-2k_2} \bar{P}, \quad \tau_{ij}^* = e^{-2k_2} \tau_{ij}, \\ \tau_{ijk}^* &= e^{-3k_2} \tau_{ijk}, \quad \overline{\frac{\partial p}{\partial x_j}}^* = e^{-3k_2} \overline{\frac{\partial p}{\partial x_j}}, \end{aligned} \quad (2.16)$$

$$\begin{aligned} \bar{T}'_s : \quad x_i^* &= x_i, \quad \bar{U}_i^* = e^{k_s} \bar{U}_i, \quad \bar{P}^* = e^{k_s} \bar{P}, \quad \tau_{ij}^* = e^{k_s} \tau_{ij} + (e^{k_s} - e^{2k_s}) \bar{U}_i \bar{U}_j, \\ \tau_{ijk}^* &= e^{k_s} \tau_{ijk} + (e^{k_s} - e^{2k_s}) (\bar{U}_i \tau_{jk} + \bar{U}_j \tau_{ik} + \bar{U}_k \tau_{ij}) \\ &\quad + (e^{k_s} - 3e^{2k_s} + 2e^{3k_s}) \bar{U}_i \bar{U}_j \bar{U}_k, \\ \overline{\frac{\partial p}{\partial x_j}}^* &= e^{k_s} \overline{\frac{\partial p}{\partial x_j}} + (e^{k_s} - e^{2k_s}) \bar{U}_i \frac{\partial \bar{P}}{\partial x_j}, \end{aligned} \quad (2.17)$$

[†]The two assumptions that the mean pressure \bar{P} decays linearly in the streamwise direction and that the mean wall-normal velocity \bar{U}_2 is constant across the channel height will be applied at a later stage.

[‡]Please note that since the system (2.9)-(2.11), or its equivalent Reynolds decomposed system (2.12)-(2.14), is unclosed even if the infinite hierarchy of equations is formally considered, all admitted invariant transformations can only be regarded in the weak sense as equivalence transformations, and not as true symmetry transformations in the strong sense. For more details, we refer to Frewer *et al.* (2014); Frewer (2015a,b) and the references therein. In the following, however, we will continue to call them imprecisely as ‘‘symmetries’’, like it was also done in Avsarkisov *et al.* (2014).

$$\begin{aligned} \bar{T}_{x_i} : \quad x_i^* &= x_i + k_{x_i}, \quad \bar{U}_i^* = \bar{U}_i, \quad \bar{P}^* = \bar{P}, \quad \tau_{ij}^* = \tau_{ij}, \\ \tau_{ijk}^* &= \tau_{ijk}, \quad \overline{u_i \frac{\partial p}{\partial x_j}}^* = \overline{u_i \frac{\partial p}{\partial x_j}}, \end{aligned} \quad (2.18)$$

$$\begin{aligned} \bar{T}_{\bar{U}_1} : \quad x_i^* &= x_i, \quad \bar{U}_1^* = \bar{U}_1 + k_{\bar{U}_1}, \quad \bar{U}_2^* = \bar{U}_2, \quad \bar{P}^* = \bar{P}, \quad \tau_{ij}^* = \tau_{ij}, \\ \tau_{ijk}^* &= \tau_{ijk}, \quad \overline{u_i \frac{\partial p}{\partial x_j}}^* = \overline{u_i \frac{\partial p}{\partial x_j}}, \end{aligned} \quad (2.19)$$

which directly follows from the set of TPC symmetries [Eqs. (3.2)-(3.6)][†] in Avsarkisov *et al.* (2014) when performing the limit of zero spatial correlation $\mathbf{r} \rightarrow \mathbf{0}$ (one-point limit) and a subsequent prolongation to higher-order moments. By equivalently rewriting the moments into their full-field form, we obtain the corresponding symmetries admitted by the reduced full-field system (2.9)-(2.11):

$$\begin{aligned} \bar{T}_1 : \quad x_i^* &= e^{k_1} x_i, \quad \bar{U}_i^* = e^{k_1} \bar{U}_i, \quad \bar{P}^* = e^{2k_1} \bar{P}, \quad \overline{U_i U_j}^* = e^{2k_1} \overline{U_i U_j}, \\ \overline{U_i U_j U_k}^* &= e^{3k_1} \overline{U_i U_j U_k}, \quad \overline{U_i \frac{\partial P}{\partial x_j}}^* = e^{2k_1} \overline{U_i \frac{\partial P}{\partial x_j}}, \end{aligned} \quad (2.20)$$

$$\begin{aligned} \bar{T}_2 : \quad x_i^* &= x_i, \quad \bar{U}_i^* = e^{-k_2} \bar{U}_i, \quad \bar{P}^* = e^{-2k_2} \bar{P}, \quad \overline{U_i U_j}^* = e^{-2k_2} \overline{U_i U_j}, \\ \overline{U_i U_j U_k}^* &= e^{-3k_2} \overline{U_i U_j U_k}, \quad \overline{U_i \frac{\partial P}{\partial x_j}}^* = e^{-3k_2} \overline{U_i \frac{\partial P}{\partial x_j}}, \end{aligned} \quad (2.21)$$

$$\begin{aligned} \bar{T}'_s : \quad x_i^* &= x_i, \quad \bar{U}_i^* = e^{k_s} \bar{U}_i, \quad \bar{P}^* = e^{k_s} \bar{P}, \quad \overline{U_i U_j}^* = e^{k_s} \overline{U_i U_j}, \\ \overline{U_i U_j U_k}^* &= e^{k_s} \overline{U_i U_j U_k}, \quad \overline{U_i \frac{\partial P}{\partial x_j}}^* = e^{k_s} \overline{U_i \frac{\partial P}{\partial x_j}}, \end{aligned} \quad (2.22)$$

$$\begin{aligned} \bar{T}_{x_i} : \quad x_i^* &= x_i + k_{x_i}, \quad \bar{U}_i^* = \bar{U}_i, \quad \bar{P}^* = \bar{P}, \quad \overline{U_i U_j}^* = \overline{U_i U_j}, \\ \overline{U_i U_j U_k}^* &= \overline{U_i U_j U_k}, \quad \overline{U_i \frac{\partial P}{\partial x_j}}^* = \overline{U_i \frac{\partial P}{\partial x_j}}, \end{aligned} \quad (2.23)$$

$$\begin{aligned} \bar{T}_{\bar{U}_1} : \quad x_i^* &= x_i, \quad \bar{U}_1^* = \bar{U}_1 + k_{\bar{U}_1}, \quad \bar{U}_2^* = \bar{U}_2, \quad \bar{P}^* = \bar{P}, \\ \overline{U_i U_j}^* &= \overline{U_i U_j} + k_{\bar{U}_1} (\delta_{1i} \bar{U}_j + \delta_{1j} \bar{U}_i) + k_{\bar{U}_1}^2 \delta_{1i} \delta_{1j}, \\ \overline{U_i U_j U_k}^* &= \overline{U_i U_j U_k} + 2 \bar{U}_i \bar{U}_j \bar{U}_k - \bar{U}_i \bar{U}_j \bar{U}_k - \bar{U}_j \bar{U}_i \bar{U}_k - \bar{U}_k \bar{U}_i \bar{U}_j \\ &\quad - 2 \bar{U}_i^* \bar{U}_j^* \bar{U}_k^* + \bar{U}_i^* \bar{U}_j \bar{U}_k^* + \bar{U}_j^* \bar{U}_i \bar{U}_k^* + \bar{U}_k^* \bar{U}_i \bar{U}_j^*, \\ \overline{U_i \frac{\partial P}{\partial x_j}}^* &= \overline{U_i \frac{\partial P}{\partial x_j}} + k_{\bar{U}_1} \delta_{1i} \frac{\partial \bar{P}}{\partial x_j}, \end{aligned} \quad (2.24)$$

which again, when performing the Reynolds decomposition (2.8), turn back into the symmetries (2.15)-(2.19). In contrast to the translation symmetry $\bar{T}_{\bar{U}_1}$ (2.24), the scaling symmetry \bar{T}'_s (2.22) gained a very simple form in the full-field representation. This so-called third scaling symmetry \bar{T}'_s in the TPC equations was first derived and discussed in Khujadze & Oberlack (2004), and only later generalized in Oberlack & Rosteck (2010) for the infinite hierarchy of MPC equations.

As we will demonstrate in detail in Section 5, since our central aim is to coherently extend the invariance analysis in Avsarkisov *et al.* (2014) to higher-order moments in which the scaling law for the lowest-order moment (mean velocity field) is based on a translation symmetry, corre-

[†]As it stands in Avsarkisov *et al.* (2014), [Eq. (3.6)] is not admitted as a symmetry by the TPC equations [Eq. (2.16)]. Only if $k_{\bar{U}_2} = 0$ it turns into a symmetry transformation. Also note that the classical translation symmetry [Eq. (3.5)] can be extended as an independent shift in all three coordinate directions.

sponding and independent translation symmetries are also needed for all higher-order moments in order to generate invariant functions with arbitrary offsets being flexible enough to match the DNS data. In other words, to be able to robustly match higher-order invariant functions to DNS data, higher-order translation symmetries are needed as they were first derived in Oberlack & Rosteck (2010).

In this regard it is worthwhile to note that the considered TPC translation symmetry [Eq.(3.6)] in Avsarkisov *et al.* (2014), does *not* correspond to the symmetry “discovered in the context of an infinite set of statistical symmetries in Oberlack & Rosteck (2010)” [p. 110], as misleadingly claimed in Avsarkisov *et al.* (2014). Instead, when adapted to the reduced one-point and full-field system (2.9)-(2.11), it is given by [Eq. (58)] in Oberlack & Rosteck (2010) as[†]

$$\begin{aligned} \bar{T}'_c: \quad x_i^* &= x_i, \quad \bar{U}_i^* = \bar{U}_i + c_i, \quad \bar{P}^* = \bar{P} + d, \quad \overline{U_i U_j}^* = \overline{U_i U_j} + c_{ij}, \\ \overline{U_i U_j U_k}^* &= \overline{U_i U_j U_k} + c_{ijk}, \quad \overline{U_i \frac{\partial P}{\partial x_j}}^* = \overline{U_i \frac{\partial P}{\partial x_j}}, \end{aligned} \quad (2.25)$$

or, in its corresponding Reynolds decomposed form, as

$$\begin{aligned} \bar{T}'_c: \quad x_i^* &= x_i, \quad \bar{U}_i^* = \bar{U}_i + c_i, \quad \bar{P}^* = \bar{P} + d, \quad \tau_{ij}^* = \tau_{ij} + \bar{U}_i \bar{U}_j - \bar{U}_i^* \bar{U}_j^* + c_{ij}, \\ \tau_{ijk}^* &= \tau_{ijk} + \bar{U}_i \bar{U}_j \bar{U}_k + \bar{U}_i \tau_{jk} + \bar{U}_j \tau_{ik} + \bar{U}_k \tau_{ij} - \bar{U}_i^* \bar{U}_j^* \bar{U}_k^* - \bar{U}_i^* \tau_{jk}^* - \bar{U}_j^* \tau_{ik}^* - \bar{U}_k^* \tau_{ij}^* + c_{ijk}, \\ \overline{u_i \frac{\partial p}{\partial x_j}}^* &= \overline{u_i \frac{\partial p}{\partial x_j}} + \bar{U}_i \frac{\partial \bar{P}}{\partial x_j} - \bar{U}_i^* \frac{\partial \bar{P}^*}{\partial x_j^*}, \end{aligned} \quad (2.26)$$

which does not reduce to (2.19), when specifying the group constants correspondingly to $c_1 = k_{\bar{U}_1}$ and $c_2 = d = c_{ij} = c_{ijk} = 0$, and which thus is the symmetry sought that independently translates all higher-order moments. In other words, the single translation symmetry (2.19) is not a “first principle” symmetry as misleadingly claimed in Avsarkisov *et al.* (2014), but was, in contrast to (2.26), rather introduced in an *ad hoc* manner just to serve the single purpose to generate a suitable logarithmic scaling law for the lowest-order moment (mean velocity field) without knowing at the same time whether this scaling is also consistent to all higher-order moments.[‡] Hence, next to the single translation symmetry (2.19), we will also apply the new “statistical translation symmetry” (2.26), first proposed in Oberlack & Rosteck (2010), in order to achieve a consistent prolongation to all higher-order moments within the symmetry analysis as particularly put forward and initialized in Avsarkisov *et al.* (2014) (see Section 5.1), and then as subsequently modified in Oberlack *et al.* (2015) (see Section 5.2).

3. On the inconsistency between the data-matched value and the theoretically predicted relation of A_1

As described in Sec. 4 in Avsarkisov *et al.* (2014), the best fit to *all* DNS data is obtained if the scaling coefficient in the theoretically derived law (1.1) is chosen as

$$A_1 = \frac{u_\tau}{0.3}. \quad (3.1)$$

Since all simulation runs in Avsarkisov *et al.* (2014) were performed under the unusual constraint of a universally fixed mean bulk velocity $U_B = U_B^*$ for different transpiration rates $v_0^+ = v_0/u_\tau$

[†]Due to the particular flow configuration considered, transformation (2.25) is only admitted as a symmetry by (2.9)-(2.11) if $c_{13} = c_{23} = c_{333} = 0$, and $c_{ij3} = 0$, for all $i \neq 3$ and $j \neq 3$.

[‡]Regarding the justification of the translation symmetry (2.19) given as [Eq.(3.6)] in Avsarkisov *et al.* (2014), it should be noted that also their statement “... that the first hint towards (3.6) has been given by Kraichnan (1965)” [p. 110], is incorrect and constitutes a misinterpretation of Kraichnan’s idea to random Galilean invariance. This misconception has been recently revealed in Frewer *et al.* (2015).

and Reynolds numbers $Re_\tau = u_\tau h / \nu$, one inevitably obtains the following parametrical dependency relationship for the mean friction velocity[†]

$$u_\tau = u_\tau(U_B^*, v_0^+, Re_\tau), \quad (3.2)$$

which for the turbulent case yet can only be determined empirically. For the laminar case, however, a closed analytical expression can be derived (see (B.10) in Appendix B). Relation (3.2) can be easily validated by taking the non-normalized definition of the mean bulk velocity [Eq. (2.4)] in Avsarkisov *et al.* (2014) and recalling the fact that due to the Navier-Stokes equations along with the supplemented boundary conditions, the mean streamwise velocity profile will in general be a function of all involved parameters of the considered flow (h : channel half-height, K : constant mean streamwise pressure gradient, v_0 : constant mean wall-normal transpiration rate, ν : kinematic viscosity):

$$U_B = \frac{1}{2h} \int_0^{2h} \bar{U}_1(x_2) dx_2 = U_B(h, K, v_0, \nu) = u_\tau \cdot \Pi(v_0^+, Re_\tau), \quad (3.3)$$

where the last relation represents its non-dimensionalized single form (relative to $u_\tau = \sqrt{|K|h}$) depending only on two dimensionless variables $v_0^+ = v_0/u_\tau$ and $Re_\tau = u_\tau h / \nu$. Note that if we universally fix $U_B = U_B^*$ in (3.3), then two of the three parameters u_τ , v_0^+ and Re_τ can be varied independently to satisfy this constraint. The third one is then predetermined by solving (3.3) for this parameter, e.g., if we choose u_τ as the dependent one, we obtain in this particular normalization the relation

$$u_\tau = \frac{U_B^*}{\Pi(v_0^+, Re_\tau)}, \quad (3.4)$$

which, of course, represents the unique dimensional reduction of its generalized expression (3.2). In Table 1 we provide the set of data obtained in Avsarkisov *et al.* (2014) to illustrate the mode of action of relation (3.4) for different turbulent flow conditions. The corresponding laminar flow cases are given as a comparison, which, in contrast to the turbulent ones, can be determined analytically, where in particular the dimensionless function Π in (3.4) can be represented even in closed form (see (B.10) in Appendix B). To note is the non-intuitive result that if v_0^+ stays fixed, u_τ monotonically decreases as Re_τ increases; a result obviously caused by the (universally fixed) constant mean bulk velocity U_B^* for these simulations.

Hence, according to (3.4), the empirically matched scaling coefficient A_1 (3.1) shows the following dependency in that it can be equivalently written as

$$A_1 = \frac{U_B^*}{0.3 \cdot \Pi(v_0^+, Re_\tau)}. \quad (3.5)$$

However, such a dependency is inconsistent to the theoretically derived result of A_1 in (1.1), which is given as

$$A_1 = \frac{k_{\bar{U}_1}}{k_1}, \quad (3.6)$$

where $k_{\bar{U}_1}$ and k_1 are two group parameters which both, due the particular symmetry analysis performed in Avsarkisov *et al.* (2014), are independent of the Reynolds number Re_τ . The reason is that the performed symmetry analysis in Avsarkisov *et al.* (2014) was done under the constraint of zero viscosity ($\nu = 0$), thus leading to a Lie-group-based derivation of A_1 (3.6), that, by construction, cannot depend on ν (or equivalently on Re_τ).

[†]That an extra parametrical relation as (3.2) is necessary to follow and to understand the numerical simulation performed, has not been directly discussed in Avsarkisov *et al.* (2014). For all simulation runs, the value U_B^* was unconventionally chosen as $U_B^* = 0.8987$. Note that this information is not given in Avsarkisov *et al.* (2014); it can only be found on their institutional data repository [fdy].

			Turbulent flow	Laminar flow
U_B^*	Re_τ	v_0^+	u_τ	u_τ^L
0.8987	250	0.05	0.0577	0.0488
0.8987	250	0.10	0.0707	0.0936
0.8987	250	0.16	0.1023	0.1475
0.8987	250	0.26	0.1861	0.2373
0.8987	250	∞		∞
0.8987	480	0.05	0.0551	0.0469
0.8987	480	0.10	0.0695	0.0918
0.8987	480	0.16	0.1004	0.1457
0.8987	480	0.26	0.1859	0.2355
0.8987	480	∞		∞
0.8987	850	0.05	0.0501	0.0460
0.8987	850	0.16	0.0980	0.1449
0.8987	∞	$v_0^+ \neq 0$		$U_B^* \cdot v_0^+$
0.8987	∞	∞		∞

Table 1: Calculated values for u_τ according to relation (3.4) for initially given U_B^* , Re_τ and v_0^+ . The latter two values were taken from Table 1 [p. 106] in Avsarkisov *et al.* (2014), while the values U_B^* and u_τ for the turbulent flow case were taken from the corresponding DNS data base disclosed by the authors on their institutional website [fdy]. The values for the corresponding laminar friction velocities u_τ^L were calculated through the analytical formula (B.11) (for given U_B^* , Re_τ and v_0^+) to serve as a comparison to the DNS-determined mean friction velocities u_τ in the turbulent case.

Although the friction velocity u_τ (3.4) only shows a rather weak Re_τ -dependence when compared to its dependence on the transpiration rate v_0^+ , as can be seen in Table 1, this dependence, however, cannot be neglected: For example, for the fixed transpiration rate $v_0^+ = 0.05$, we have a change of nearly 15% in u_τ when increasing the Reynolds number from $Re_\tau = 250$ to 850. This change in u_τ (3.4) is then directly reflected in A_1 according to its empirical relation (3.5) proposed in Avsarkisov *et al.* (2014). And this change will continue to grow when increasing the Reynolds number even further. But, as we can observe from the corresponding laminar values u_τ^L in Table 1, this growth is bounded, i.e., for $Re_\tau \rightarrow \infty$ the values for u_τ will converge to some certain finite value u_τ^∞ , which is also expected to happen in the turbulent case since the flow is arranged under the same unusual condition of a universally fixed bulk velocity U_B^* :

$$\lim_{Re_\tau \rightarrow \infty} u_\tau = \lim_{Re_\tau \rightarrow \infty} \frac{U_B^*}{\Pi(v_0^+, Re_\tau)} = \frac{U_B^*}{\Pi_\infty(v_0^+)} = u_\tau^\infty, \text{ for } 0 < v_0^+ < \infty. \quad (3.7)$$

In contrast to the laminar case, where this value is analytically accessible and particularly given as $u_\tau^\infty = U_B^* v_0^+$, it is, of course, an unknown quantity for the turbulent case; yet still, it will take a different (most possibly lower) value than for any finite Reynolds number $Re_\tau < \infty$.

Although weak, the friction velocity u_τ (3.4), and thus also the empirically matched logarithmic scaling coefficient A_1 (3.5), nevertheless shows a non-negligible Re_τ -dependence for every initially fixed transpiration rate v_0^+ , a dependence which, as we will demonstrate in Section 5.1, is critical when extending the symmetry analysis as put forward in Avsarkisov *et al.* (2014) to higher-order moments.

Hence, the central assumption in Avsarkisov *et al.* (2014) to predict the (non-normalized) mean velocity scaling behavior in the center of the channel by an invariant log-law resulting from a non-viscous ($\nu = 0$) symmetry analysis, namely by (1.1) where A_1 and B_1 are independent on

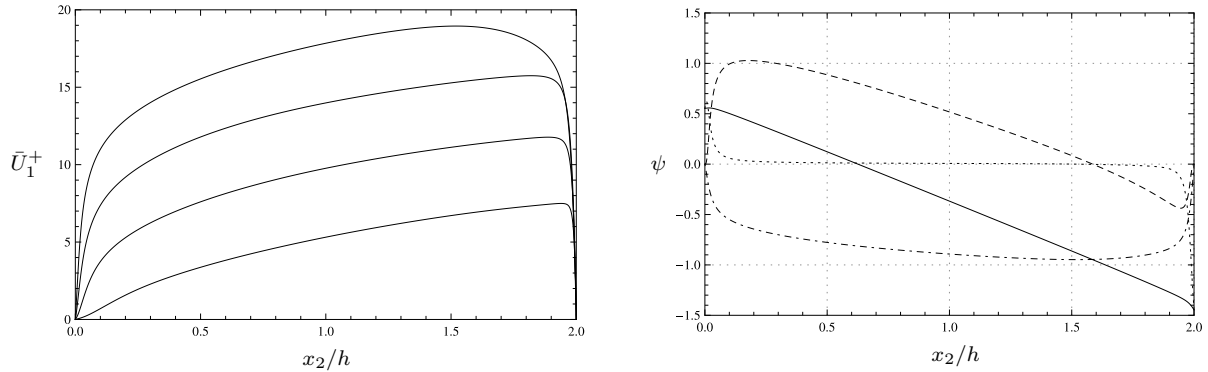


Figure 1: Reproduction of Fig. 3 (a) and (c) in Avsarkisov *et al.* (2014) with the data provided by the authors on their institutional website [fdy]. *Left plot:* Mean streamwise velocity profile \bar{U}_1^+ at $Re_\tau = 480$ for $v_0^+ = 0.05, 0.1, 0.16$ and 0.26 (from top to bottom). *Right plot:* The quantity ψ displays different shear stress distributions at $Re_\tau = 480$ for the fixed transpiration rate $v_0^+ = 0.05$: $-\overline{u_1 u_2^+}$ (---); $-v_0^+ \bar{U}_1^+$ (- · - ·); $d\bar{U}_1^+/dx_2^+$ (···); $\tau^+ - v_0^+ \bar{U}_1^+$ (—), where $\tau^+ = -\overline{u_1 u_2^+} + d\bar{U}_1^+/dx_2^+$ is the total shear stress without transpiration as defined in [Eq. (2.11)] in Avsarkisov *et al.* (2014). The differences in this right plot to Fig. 3 (c) are of minor significance: (i) The small numerical error (misfeature) at the wall boundaries in the profile $\tau^+ - v_0^+ \bar{U}_1^+$ (solid line) has not been displayed in Fig. 3 (c). Across the full channel height, a pure straight line with the same slope of measure one has been given instead, i.e., the true profile of this quantity has not been plotted in Avsarkisov *et al.* (2014). (ii) A careful comparison reveals a very small discrepancy in the vertical position of both the dashed-dotted and the solid line. This negligible difference may be explained by the circumstance that the data base on the author’s website may refer to a different, most possibly to a newer simulation run with a better statistics than the one presented in Avsarkisov *et al.* (2014): The latter version was published in January 2014, while the released data base on their website was created a year later in February 2015. Nevertheless, both plots above show that Fig. 3 (a) and (c) in Avsarkisov *et al.* (2014) are reproducible, confirming thus that we are using the correct data set.

Re_τ , is not justified. For that, a viscous ($\nu \neq 0$) symmetry analysis has to be performed, but then, as we will consequently show in Section 5.2, no invariant mean velocity profile for \bar{U}_1 can be constructed anymore,[†] due to the well-known (scaling) symmetry breaking mechanism of the viscous terms.

4. On the problems when trying to reproduce Figure 9

In this section we show the results of our effort to reproduce Figs. 9 (a) and (c) in Avsarkisov *et al.* (2014). The underlying simulation data were taken from the author’s institutional website [fdy]. To verify and to ensure that we operate with the same data set as presented in Avsarkisov *et al.* (2014), we first have to check if we are able to repeat the construction of another figure. By choosing Figs. 3 (a) and (c) as representative test cases, our reproduced plots in Figure 1 undoubtedly show that we are indeed in hold of the correct simulation data to systematically investigate the reproducibility of all plots in Avsarkisov *et al.* (2014).

Hence, the result of Figure 1 allows us to make the conclusion that both Figs. 9 (a) and (c) in Avsarkisov *et al.* (2014) are *not* reproducible, when considering our reproduction in Figure 2 and Figure 3, respectively.

[†]Except only for a linear profile (5.40) as derived in Section 5.2, but which, of course is not a reasonable turbulent scaling law. To note is that in Oberlack *et al.* (2015) the authors succeeded to derive both a logarithmic as well as an algebraic scaling law for the mean velocity field in the viscous case. But, as we will analytically prove in Section 5.2, both results are based on a methodological mistake. This is also expressed in the fact that as we repeat their inconsistent analysis, certain higher order moments cannot be matched to the DNS data.

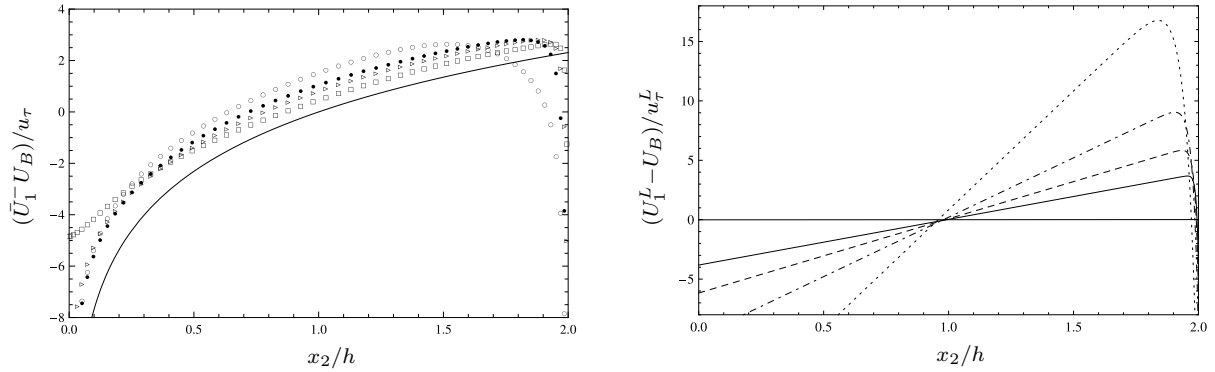


Figure 2: *Left plot:* Reproduction of Fig.9 (a) in Avsarkisov *et al.* (2014) with the data provided by the authors on their institutional website [fdy]. For constant Reynolds number $Re_\tau = 480$, the mean velocity profile in deficit form is displayed for different transpiration rates: $v_0^+ = 0.05$ (\circ); $v_0^+ = 0.10$ (\bullet); $v_0^+ = 0.16$ (\triangleright); $v_0^+ = 0.26$ (\square). For all cases the mean bulk velocity U_B (3.3) takes the universal value $U_B = U_B^*$, where $U_B^* = 0.8987$; in contrast to the values for u_τ , which are not universal (see Table 1 for the corresponding values). The solid line displays the new (theoretically predicted) logarithmic scaling law (1.2) for the parameters $\gamma = 0.3$, $B_1 = 0$ and $C_1 = U_B$ as proposed in Sec.4 in Avsarkisov *et al.* (2014). Obviously, a comparison to Fig.9 (a) readily reveals that this figure is not reproducible. It shows a strong discrepancy in two independent aspects with the effect that an overall opposite conclusion is obtained than as proposed in Avsarkisov *et al.* (2014). For more details, see the main text.

Right plot: To have a qualitative comparison to the turbulent case, we plotted the corresponding laminar profiles for the same external parameters as were used in the figure on the left-hand side. From top to bottom (relative to the positive function values), the corresponding laminar profile structure is displayed for increasing transpiration rates $v_0^+ = 0.05, 0.1, 0.16, 0.26$ at fixed $Re_\tau = 480$ and $U_B = U_B^* = 0.8987$. The associated values for the laminar friction velocities u_τ^L can be taken from Table 1, which are based on the closed analytical expression for the laminar velocity profile U_1^L (B.11). See the main text for a comparative discussion between the turbulent case (left plot) and its corresponding laminar case (right plot).

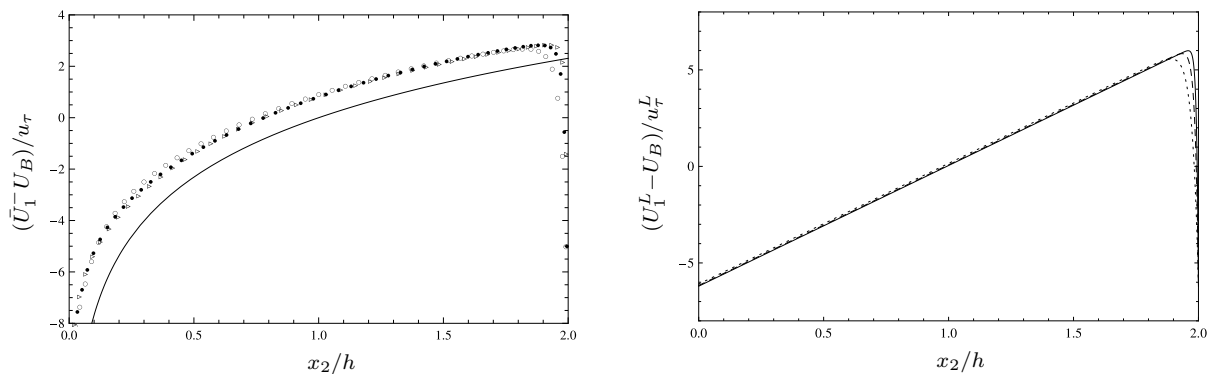


Figure 3: *Left plot:* Reproduction of Fig.9 (c) in Avsarkisov *et al.* (2014) with the data provided by the authors on their institutional website [fdy]. In the same way as in Figure 2, the mean velocity profile in deficit form is again displayed, but now at a constant transpiration rate $v_0^+ = 0.16$ for different Reynolds numbers: $Re_\tau = 250$ (\circ); $Re_\tau = 480$ (\bullet); $Re_\tau = 850$ (\triangleright). The solid line displays again the new (theoretically predicted) logarithmic scaling law (1.2) for the corresponding parameters $\gamma = 0.3$, $B_1 = 0$ and $C_1 = U_B$, as proposed in Sec.4 in Avsarkisov *et al.* (2014) also for this case.

Right plot: For the same motivation as in Figure 2, the corresponding laminar deficit profiles are plotted. From left to right the Reynolds number increases $Re_\tau = 250, 480, 850$ at fixed transpiration rate $v_0^+ = 0.16$ and bulk velocity $U_B = U_B^* = 0.8987$. The laminar velocity profile U_1^L and its associated consistent friction velocity u_τ^L are given through the analytical expressions of (B.11); the explicit values of u_τ^L for the considered parameter combinations are given again in Table 1. For a comparative discussion between the turbulent case (left plot) and its corresponding laminar case (right plot), see again the main text.

4.1. The nonreproducibility of Figure 9 (a)

Comparing our left plot in Figure 2 with the corresponding Fig. 9 (a) in Avsarkisov *et al.* (2014), readily reveals that this figure is not reproducible. It shows a strong discrepancy in two independent aspects with the effect that an overall opposite conclusion is obtained than as proposed in Avsarkisov *et al.* (2014): (i) The DNS data for the mean streamwise velocity at a fixed Reynolds number and varying transpiration rates, do *not* universally collapse onto one single curve when formulated in its deficit form. Instead we see a monotonous decay of the profile as the transpiration rate increases. (ii) The theoretically predicted scaling law (solid line) does not match the data, not even in a rough approximate sense. For that different matching parameters need to be formulated. If B_1 is continued to be chosen as zero, then both γ and C_1 need to be functions of v_0^+ , where it should be noted that for higher transpiration rates the matching region shifts to the suction wall $x_2/h = 2$.

The right plot in Figure 2 serves as a comparative reference to the left one. It allows to compare the differences and similarities between the laminar and the turbulent flow behavior. For the same external parameters as were used for the turbulent case, this plot shows the corresponding laminar profiles derived in analytically closed form in Appendix B, with the final result given in (B.11). Interesting to see is how the deficit profile at a constant finite Reynolds number decays for increasing transpiration rates until it globally goes to zero when reaching the limit $v_0^+ \rightarrow \infty$ (since in this limit $u_\tau^L \rightarrow \infty$ and $|U_1^L| < 2U_B^*$, in particular $u_\tau \rightarrow U_B^* v_0^+$ and thus $U_1^L \rightarrow U_B^* \cdot x_2/h$, for $0 \leq x_2/h < 2$). A similar behavior, although based on a more complex functional structure, is also to be expected for the turbulent case:[†] Indeed, in the left plot the onset of this global tendency in the DNS data can already be positively observed.

4.2. The nonreproducibility of Figure 9 (c)

Comparing now the left plot of Figure 3 with the corresponding Fig. 9 (c) in Avsarkisov *et al.* (2014), we see that although the DNS data in this case more or less universally collapses onto a single curve and also coincides with the representation and conclusion in Avsarkisov *et al.* (2014), the new logarithmic scaling law (1.2) (solid line), however, still does not match the data for the proposed parameters $\gamma = 0.3$, $B_1 = 0$ and $C_1 = U_B$. For an unaltered γ , a vertical upward shift of at least 0.82 units is needed, i.e., in order to match the data, the integration constant C_1 needs to be modified from $C_1 = U_B$ at least to $C_1 = U_B + 0.82 \cdot u_\tau$, a result not obtained in Avsarkisov *et al.* (2014). Hence, we may correctly claim that also Fig. 9 (c) is not reproducible.

As in Figure 2, the corresponding laminar deficit profiles are presented and studied in the right plot of Figure 3. Interesting to see here is that by close inspection the deficit profiles at a constant transpiration rate do not really collapse onto a single curve, but rather, within the range $0 \leq x_2/h < 2$, slowly converge to a particular linear profile in the limit of infinite Reynolds number $Re_\tau \rightarrow \infty$. Note that this convergence takes place pointwise, i.e., the points close to the blowing wall ($x_2/h = 0$) converge exponentially faster than those points close to the suction wall ($x_2/h = 2$), due to the presence of a boundary layer at this side. In particular, the deficit profile converges to $(U_1^L - U_B^*)/u_\tau^L \rightarrow 1/v_0^+ \cdot x_2/h - 1/v_0^+$, for $0 \leq x_2/h < 2$, i.e., equivalently as in the previous section for a fixed Reynolds number, the laminar velocity profile in this range converges again to $U_1^L \rightarrow U_B^* \cdot x_2/h$, since in this case for a fixed transpiration rate $u_\tau^L \rightarrow U_B^* \cdot v_0^+$; see (B.11). A similar behavior, although based on a more complex functional structure, is also to be expected for the turbulent case: Indeed, by close inspection of the left plot of Figure 3, one can observe that everywhere throughout the channel, the DNS data does not universally lie on a single curve as claimed in Avsarkisov *et al.* (2014), but that in fact for increasing Reynolds number a (slow) pointwise convergence towards a particular profile takes place.

[†]Note that global laminar flow properties are most probably also statistically featured by the corresponding turbulent flow condition and thus also to be expected in a qualitative sense. The opposite conclusion, however, is of course not true: A turbulent flow may statistically show additional features that are not existent in its associated laminar base flow.

5. On the inconsistency of the Lie-group-based scaling theory in turbulence

In this section we will reveal the fact that when coherently extending the Lie-group-based scaling theory as presented in Avsarkisov *et al.* (2014) for the newly proposed logarithmic law [Eq. (3.16)] to higher orders of the one-point velocity correlations, one unavoidably runs into a fundamental inconsistency in that one fails to match certain theoretically derived scaling laws to the given DNS data. We will investigate both the inviscid (Euler, $\nu = 0$) case, as particularly realized in Avsarkisov *et al.* (2014), as well as the viscous (Navier-Stokes, $\nu \neq 0$) case, as subsequently modified in Oberlack *et al.* (2015). To simplify formal expressions and calculations, we will derive all theoretical results in the full-field (instantaneous) representation. The corresponding Reynolds decomposed results (later needed to directly compare to the DNS data) are then obtained straightforwardly by just performing the decomposition (2.8). To demonstrate our point in this section, it is fully sufficient to only consider the turbulent transport equations up to second order, since they already involve (unclosed) third order moments for which the inconsistency to the DNS data is clearly pronounced.

5.1. The inviscid case ($\nu = 0$)

The governing one-point equations for the flow considered in Avsarkisov *et al.* (2014) are given by the system (2.9)-(2.11), which, as discussed in Section 2, admits the continuous set of Lie-point symmetries (2.20)-(2.24) and (2.25), where the latter symmetry is needed to appropriately extend the construction of invariant solutions in Avsarkisov *et al.* (2014) to higher-order moments. Hence, when combining all symmetries and following the line of reasoning in Avsarkisov *et al.* (2014), we obtain the following invariant surface condition

$$\begin{aligned}
\frac{dx_1}{k_1 x_1 + k_{x_1}} &= \frac{dx_2}{k_1 x_2 + k_{x_2}} = \frac{d\overline{U}_i}{(k_1 - k_2 + k_s)\overline{U}_i + \kappa_i + c_i} = \frac{d\overline{P}}{(2k_1 - 2k_2 + k_s)\overline{P} + \kappa^p + d} \\
&= \frac{d(\partial_i \overline{P})}{(k_1 - 2k_2 + k_s)\partial_i \overline{P} + \kappa_i^p} = \frac{d\overline{U}_i \overline{U}_j}{(2k_1 - 2k_2 + k_s)\overline{U}_i \overline{U}_j + \kappa_{ij} + c_{ij}} \\
&= \frac{d\overline{U}_i \overline{U}_j \overline{U}_k}{(3k_1 - 3k_2 + k_s)\overline{U}_i \overline{U}_j \overline{U}_k + \kappa_{ijk} + c_{ijk}} \\
&= \frac{d\overline{U}_i \partial_j \overline{P}}{(2k_1 - 3k_2 + k_s)\overline{U}_i \partial_j \overline{P} + \kappa_{ij}^p}, \tag{5.1}
\end{aligned}$$

which coherently extends their corresponding condition [Eq. (3.12)] up to third order including the pressure moments. The functional κ -extensions result from the single translation symmetry $\overline{T}_{\overline{U}_1}$ (2.19) when written in its equivalent full-field form (2.24), and are thus given as[†]

$$\left. \begin{aligned}
\kappa_i &= k_{\overline{U}_1} \delta_{1i}, & \kappa_{ij} &= \kappa_i \overline{U}_j + \kappa_j \overline{U}_i, \\
\kappa_{ijk} &= \kappa_{ij} \overline{U}_k + \kappa_{ik} \overline{U}_j + \kappa_{jk} \overline{U}_i \\
&\quad + \kappa_i (\overline{U}_j \overline{U}_k - 2\overline{U}_j \overline{U}_k) + \kappa_j (\overline{U}_i \overline{U}_k - 2\overline{U}_i \overline{U}_k) + \kappa_k (\overline{U}_i \overline{U}_j - 2\overline{U}_i \overline{U}_j), \\
\kappa^p &= 0, & \kappa_i^p &= 0, & \kappa_{ij}^p &= \kappa_i \frac{\partial \overline{P}}{\partial x_j}.
\end{aligned} \right\} \tag{5.2}$$

Progressively, we will now determine all invariant functions from (5.1) and examine in how far they are compatible to the underlying equations (2.9)-(2.11). The first step in this procedure

[†]Note that the quadratic term $k_{\overline{U}_1}^2 \delta_{1i} \delta_{1j}$ in the transformation $\overline{T}_{\overline{U}_1}$ (2.24) for $\overline{U}_i \overline{U}_j$ is not contributing in its local (infinitesimal) generator, since Lie-group symmetry theory is a linear theory where all information of the transformations is carried in the linear expansion terms of the group parameters.

is to ensure the invariance of any existing constraints. We recall the two constraints of a mean constant wall-normal velocity $\overline{U_2} = v_0$, or, equivalently $d\overline{U_2} = 0$, and that of a mean constant streamwise pressure gradient $\partial\overline{P}/\partial x_1 = -K$, or, equivalently $d(\partial_1\overline{P}) = 0$. Implementing the first constraint $d\overline{U_2} = 0$ into (5.1) will consequently result into the corresponding combined symmetry breaking constraint[†]

$$k_1 - k_2 + k_s = 0, \quad \text{and} \quad c_2 = 0, \quad (5.3)$$

as discussed and implemented in Avsarkisov *et al.* (2014). The second constraint $d(\partial_1\overline{P}) = 0$, however, will result into an additional symmetry breaking constraint

$$k_1 - 2k_2 + k_s = 0, \quad (5.4)$$

which was *not* discussed in Avsarkisov *et al.* (2014); an important result indeed, since, due to (5.3), it equivalently turns into the strong constraint

$$k_2 = 0. \quad (5.5)$$

Note that this result could have also been obtained when directly solving from condition (5.1) the invariant function for the pressure \overline{P} as a function of x_1 and x_2 along with the first constraint of (5.3). Because, this result, when taking its gradient in the streamwise direction,

$$\frac{\partial\overline{P}(x_1, x_2)}{\partial x_1} = F_1\left(\frac{x_1 + k_{x_1}/k_1}{x_2 + k_{x_2}/k_1}\right) \cdot (x_2 + k_{x_2}/k_1)^{-k_2/k_1}, \quad (5.6)$$

obviously, is only compatible to

$$\frac{\partial\overline{P}(x_1, x_2)}{\partial x_1} = -K, \quad (5.7)$$

if the integration function F_1 is a global constant equal to $-K$, and, if $k_2 = 0$. Collecting now all obtained symmetry breaking constraints

$$k_2 = 0, \quad k_s = -k_1, \quad c_2 = 0, \quad (5.8)$$

and applying them to the originally formulated condition (5.1), will drastically restrict the possible structures for the considered invariant functions. For example, for the mean streamwise velocity profile $\overline{U_1}$ only a logarithmic function of the form

$$\overline{U_1}(x_2) = A_1 \ln\left(\frac{x_2}{h} + B_1\right) + C_1, \quad (5.9)$$

is possible, where C_1 is an arbitrary integration constant and $A_1 = (k_{\overline{U_1}} + c_1)/k_1$, $B_1 = k_{x_2}/(k_1 h)$ two independent parameters uniquely determined by internal group constants. But, not only the symmetry breaking constraints, also the underlying dynamical equations of the considered system restrict the functions (for ODEs) or the functional possibilities (for PDEs) even further, for example, when considering the full derivation of the invariant correlation $\overline{U_1 U_2}$: From the defining condition (5.1) with inserted constraints (5.8) it is initially given by

$$\overline{U_1 U_2}(x_2) = C_{12} \left(\frac{x_2}{h} + B_1\right) + \tilde{A}_{12}, \quad (5.10)$$

where C_{12} is again some arbitrary integration constant, and where $\tilde{A}_{12} = -(k_{\overline{U_1}} v_0 + c_{12})/k_1$, like $B_1 = k_{x_2}/(k_1 h)$, is a parameter that, apart from the external system parameter v_0 , comprises again internal group constants.[‡] However, the arbitrariness of C_{12} is illusive, because the

[†]Note that both constraints in (5.3) are necessary to avoid an overall zero surface condition (5.1).

[‡]That the parameter \tilde{A}_{12} includes the external system parameter v_0 , is denoted by the “tilde” symbol. With the notation introduced in (5.12), this parameter can also be written as $\tilde{A}_{12} = A_{12} + A_0 v_0$, where $A_{12} = -c_{12}/k_1$ and $A_0 = -k_{\overline{U_1}}/k_1$ are then two parameters determined by internal group parameters only. This notation will also be used later in (5.15) when matching the invariant functions to DNS data, where the “tilde” symbol denotes essential fitting parameters collecting all constants, independent of their nature, into a single expression.

underlying momentum equation (2.10) restricts it to

$$C_{12} = K \cdot h. \quad (5.11)$$

All remaining invariant functions can then be generically determined as

$$\left. \begin{aligned} \overline{U_i U_j}(x_2) &= C_{ij} \left(\frac{x_2}{h} + B_1 \right) + A_0 \delta_{ijk} \overline{U_k} + A_{ij}, & \overline{U_1 U_3}(x_2) &= \overline{U_2 U_3}(x_2) = 0, \\ \overline{U_i U_j U_k}(x_2) &= C_{ijk} \left(\frac{x_2}{h} + B_1 \right)^2 + \frac{A_0}{2} \delta_{ijkmn} \left[C_{mn} \left(\frac{x_2}{h} + B_1 \right) + \overline{U_m U_n}(x_2) \right] + A_{ijk}, \\ \partial_2 \overline{P}(x_1, x_2) &= C^p, & \overline{U_i \partial_j P}(x_2) &= C_{ij}^p \left(\frac{x_2}{h} + B_1 \right) - A_0 (\delta_{1i} \delta_{1j} K - \delta_{1i} \delta_{2j} C^p), \end{aligned} \right\} \quad (5.12)$$

where the C -parameters are arbitrary integration constants, while the A -parameters are determined through the group constants as

$$\left. \begin{aligned} A_0 &= -\frac{k \bar{U}_1}{k_1}, & A_1 &= \frac{k \bar{U}_1 + c_1}{k_1}, & A_{ij} &= 2A_0 A_1 \delta_{1i} \delta_{1j} - \frac{c_{ij}}{k_1}, \\ A_{ijk} &= \frac{3}{2} A_0^2 A_1 \delta_{1i} \delta_{1j} \delta_{1k} - \frac{c_{ijk}}{2k_1}, \end{aligned} \right\} \quad (5.13)$$

and, finally, the modified δ -functions in (5.12) are defined as

$$\left. \begin{aligned} \delta_{ijk} &= \delta_{1i} \delta_{jk} + \delta_{1j} \delta_{ik}, \\ \delta_{ijkmn} &= \frac{\delta_{1i}}{2} (\delta_{jm} \delta_{kn} + \delta_{jn} \delta_{km}) + \frac{\delta_{1j}}{2} (\delta_{im} \delta_{kn} + \delta_{in} \delta_{km}) + \frac{\delta_{1k}}{2} (\delta_{im} \delta_{jn} + \delta_{in} \delta_{jm}). \end{aligned} \right\} \quad (5.14)$$

The arbitrary integration constants, however, are not fully independent but show certain fixed interrelations resulting from the underlying transport equations (2.9)-(2.11) that the invariant functions need to satisfy, e.g., $C^p = -C_{22}/h$, or $2C_{122}/h + C_{12}^p + C_{21}^p = 0$. When Reynolds decomposing all derived invariant results, we straightforwardly obtain[†]

$$\left. \begin{aligned} \bar{U}_1 &= A_1 \ln \left(\frac{x_2}{h} + B_1 \right) + C_1, & \bar{U}_2 &= v_0, & \tau_{13} &= \tau_{23} = 0, \\ \tau_{11} &= C_{11} \left(\frac{x_2}{h} + B_1 \right) - \bar{U}_1^2 + 2A_0 \bar{U}_1 + A_{11}, & \tau_{12} &= u_\tau^2 \left(\frac{x_2}{h} + B_1 \right) - v_0 \bar{U}_1 + \tilde{A}_{12}, \\ \tau_{22} &= C_{22} \left(\frac{x_2}{h} + B_1 \right) + \tilde{A}_{22}, & \tau_{33} &= C_{33} \left(\frac{x_2}{h} + B_1 \right) + A_{33}, \\ \tau_{112} &= C_{112} \left(\frac{x_2}{h} + B_1 \right)^2 + 2A_0 u_\tau^2 \left(\frac{x_2}{h} + B_1 \right) - 2\bar{U}_1 \tau_{12} - v_0 \tau_{11} - v_0 \bar{U}_1^2 + \tilde{A}_{112}, \\ \tau_{222} &= C_{222} \left(\frac{x_2}{h} + B_1 \right)^2 - 3v_0 \tau_{22} + \tilde{A}_{222}, & \tau_{233} &= C_{233} \left(\frac{x_2}{h} + B_1 \right)^2 - v_0 \tau_{33} + A_{233}, \end{aligned} \right\} \quad (5.15)$$

which then can be validated against the given DNS data. Note that we only listed those functions for which the statistical data has been made available from the DNS in Avsarkisov *et al.* (2014). For the scaling factor (5.11) we used the central definition $u_\tau^2 = K \cdot h$ (see [Eq. (2.1)]). When fitting the set of functions (5.15) to the data, special attention has to be paid to the invariant scaling laws for τ_{11} , τ_{12} and τ_{112} , which all show a combination of an algebraic and a logarithmic scaling, an awkward property, which again only has its origin in the new statistical symmetries \bar{T}'_s (2.22) and \bar{T}'_c (2.25) first proposed in Oberlack & Rosteck (2010).

[†]The four ‘‘tilde’’-parameters are given as: $\tilde{A}_{12} = v_0 A_0 + A_{12}$, $\tilde{A}_{22} = -v_0^2 + A_{22}$, $\tilde{A}_{222} = -v_0^3 + A_{222}$, and $\tilde{A}_{112} = A_0 \tilde{A}_{12} + A_{112}$.

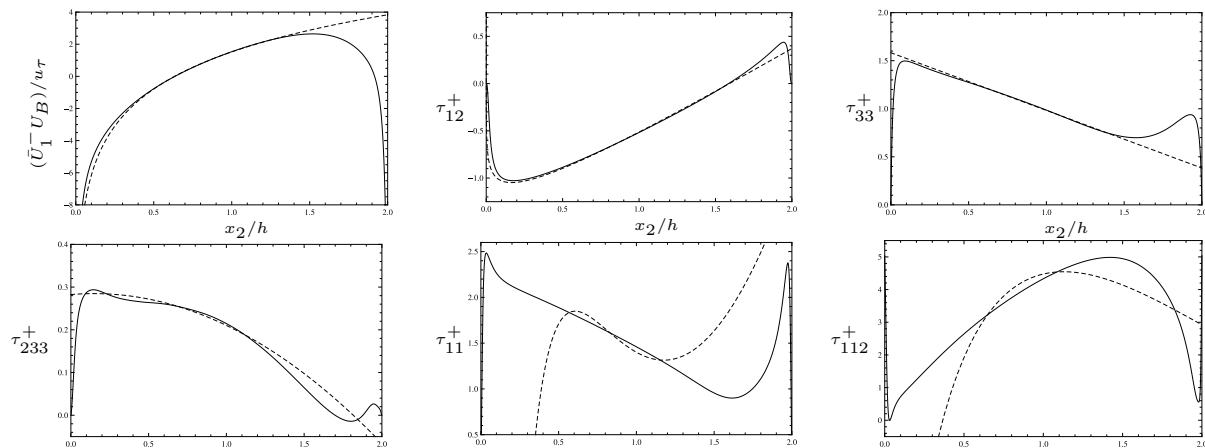


Figure 4: Matching of the theoretically predicted scaling laws (5.15) to the DNS data for $Re_\tau = 480$ and $v_0^+ = 0.05$. The DNS data is displayed by solid lines, the corresponding scaling laws by dashed lines. The associated parameters for this best fit in each case can be taken from Table 2, where the matching region was chosen in the range $0.50 \leq x_2/h \leq 1.25$. For more details and a discussion on the fitting results obtained, see the main text.

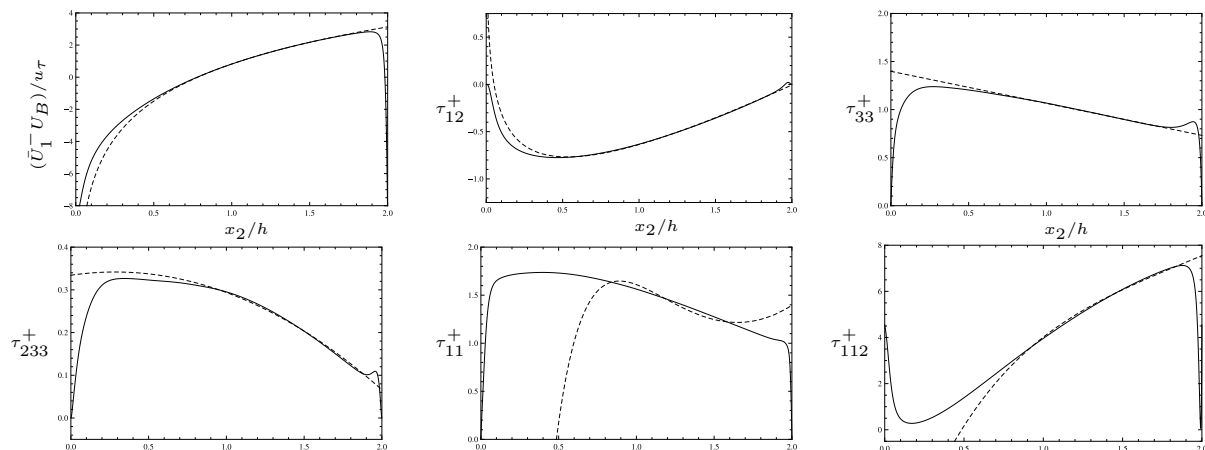


Figure 5: Matching of the theoretically predicted scaling laws (5.15) to the DNS data for the same Reynolds number $Re_\tau = 480$ as in the figure given above, but for a higher transpiration $v_0^+ = 0.16$. The DNS data is again displayed by solid lines, the corresponding scaling laws by dashed lines. The associated best-fitted parameters can be taken again from Table 2, where the matching region was now set differently in the range $0.75 \leq x_2/h \leq 1.70$. For more details and a comparative discussion on the fitting results obtained between the lower (Figure 4) and the higher transpiration case (Figure 5), see again the main text.

Figure 4 & 5 show the matching of the analytically (from “first principles”) derived scaling laws (5.15) to the DNS data at $Re_\tau = 480$ for the two different transpiration rates $v_0^+ = 0.05$ and $v_0^+ = 0.16$, respectively. The matching was performed in the u_τ -normalization, i.e., for the normalized velocity correlations $\tau_{ij}^+ = \tau_{ij}/u_\tau^2$ and $\tau_{ijk}^+ = \tau_{ijk}/u_\tau^3$, as well as for the normalized mean velocity field in its deficit form $(\bar{U}_1 - U_B)/u_\tau = \bar{U}_1^+ - U_B^+$. The particular values for u_τ as well as for $U_B = U_B^*$ in each case can be taken from Table 1.

The matching region in Figure 4 was chosen in the range $0.50 \leq x_2/h \leq 1.25$, based on the best fit regarding the central prediction in Avsarkisov *et al.* (2014), namely that of a new logarithmic scaling law (1.2) for the mean velocity field in the center of the channel

$$\frac{\bar{U}_1 - U_B}{u_\tau} = \frac{1}{\gamma} \ln(x_2/h) + \lambda, \quad (5.16)$$

v_0^+	$\frac{\bar{U}_1 - U_B}{u_\tau}$		τ_{12}^+	τ_{33}^+		τ_{233}^+		τ_{11}^+		τ_{112}^+	
	γ	λ	\tilde{A}_{12}^+	A_{33}^+	C_{33}^+	A_{233}^+	C_{233}^+	A_{11}^+	C_{11}^+	\tilde{A}_{112}^+	C_{112}^+
0.05	0.3	1.524	-0.622	1.583	-0.600	0.362	-0.102	-199.1	25.85	-28.34	2.854
0.16	0.3	0.821	-0.074	1.398	-0.333	0.558	-0.094	-57.20	18.05	-10.14	3.307

Table 2: Best-fitted parameters of the theoretically predicted scaling laws (5.15) to the DNS data as shown in Figure 4 & 5 for two different transpiration rates $v_0^+ = 0.05$ and $v_0^+ = 0.16$, respectively, at $Re_\tau = 480$. The parameter A_0^+ was fitted for τ_{11}^+ , and then applied in τ_{112}^+ : It takes the value $A_0^+ = 13.82$ for $v_0^+ = 0.05$, and $A_0^+ = 6.971$ for $v_0^+ = 0.16$. The matching region for the lower rate $v_0^+ = 0.05$ was chosen in the range $0.50 \leq x_2/h \leq 1.25$, while for the higher rate $v_0^+ = 0.16$ it was determined to lie in the range $0.75 \leq x_2/h \leq 1.70$. For more details, see the main text.

with the fixed universal scaling coefficient $\gamma = 0.3$ referring to (1.3). Note that in Avsarkisov *et al.* (2014) no additional vertical shift λ was needed, but which, as we have demonstrated before, only leads to non-reproducible results (see Section 4, in particular the discussion on the nonreproducibility of Fig. 9 (c) in Avsarkisov *et al.* (2014)). Depending on the transpiration rate and the Reynolds number, a constant vertical upward shift $\lambda > 0$ is necessary to match the DNS data. Its presence, of course, re-defines the proposed integration constant in (1.3) as $C_1 = U_B + \lambda \cdot u_\tau$, turning thus C_1 into a *non*-universal constant, depending then on both the Reynolds number Re_τ and the transpiration rate v_0^+ , where the latter dependency is more pronounced than the former one. A result opposite to the one claimed in Avsarkisov *et al.* (2014), where C_1 was determined as a universal constant, with the particular value $C_1 = U_B$ (1.3) for a universally fixed bulk velocity $U_B = U_B^*$ as it is explicitly given in Table 1.

Based on the matching region in Figure 4, the corresponding region for the higher transpiration rate in Figure 5 was determined to lie in the range $0.75 \leq x_2/h \leq 1.70$. This range was determined such that it has the same absolute residual range $-0.015 \leq y_s - f_m(x_2/h) \leq 0.015$ as the one chosen for the lower transpiration rate in Figure 4 when fitting the central scaling law (5.16), where $y_s = (\bar{U}_1 - U_B)/u_\tau$ are the simulated (DNS) values and $f_m(x_2/h) = \ln(x_2/h)/\gamma + \lambda$ the values from the considered model function.[†] Such a procedure is necessary if one is interested in how an initially chosen matching region changes when varying any external system parameters. When comparing the matching region $0.50 \leq x_2/h \leq 1.25$ for $v_0^+ = 0.05$ in Figure 4, with the corresponding region $0.75 \leq x_2/h \leq 1.70$ for $v_0^+ = 0.16$ in Figure 5, we clearly observe that as the transpiration rate moderately increases at constant Reynolds number (up to $v_0^+ \leq 0.16$), the matching region not only grows in extent, but that it also, at the same time, shifts to the right towards the suction wall ($x_2/h \rightarrow 2$). An important result which again has not been indicated in Avsarkisov *et al.* (2014). Instead, only the first property of a growing validity region is reported, which, however, cannot be true as a single statement for ever increasing transpiration rates: In fact, since for higher rates the validity region also shifts more and more to the fixed right-hand boundary at the suction wall, it eventually has to revert this growing trend at a certain transpiration rate high enough. For example, the rate $v_0^+ = 0.26$ (at $Re_\tau = 480$) is already sufficient to demonstrate a *non*-increased validity region when compared to all lower rates at the same Reynolds number. Based on the same (residual) condition as for the considered lower rates, the matching region for $v_0^+ = 0.26$ reduced to $1.35 \leq x_2/h \leq 1.80$, where at the same time a strong shift to the right (suction side) has occurred.

[†]Hence, by construction, the quality of the fit for the mean velocity profile \bar{U}_1 in Figure 5 is thus the same as in Figure 4. As a result, the mean velocity profile provided in each case the necessary but *a priori* unknown matching region, which now serves as a basis to systematically fit all remaining velocity correlations to the DNS data. The best-fitted parameter values for the correlations functions (5.15) are listed in Table 2.

In the following (comparative) discussion on the quality of the fits for the velocity correlations τ_{ij}^+ and τ_{ijk}^+ in Figure 4 & 5, we will only focus on the systematic failure when fitting scaling laws which show a simultaneous combination of an algebraic and a logarithmic scaling. The fitted correlation functions in (5.15) can be separated into two classes: Those which show a strong (at least quadratic) dependency on the mean streamwise velocity field \bar{U}_1 , as τ_{11}^+ and τ_{112}^+ , and those which only show a weak (at most linear) or no dependency at all on this field, as the remaining ones in this list: τ_{12}^+ , τ_{33}^+ and τ_{223}^+ . While the latter correlations more or less satisfactorily match the DNS data (where the lower order correlations τ_{12}^+ and τ_{33}^+ show a better matching than the higher order one τ_{223}^+), the fitting of the former correlations τ_{11}^+ and τ_{112}^+ fails to predict the tendency of the data.

Based on our previous studies Frewer *et al.* (2014, 2015) supplemented by Frewer (2015c) and Frewer *et al.* (2016), several different mathematical proofs are given that explain this failure and discrepancy in the matching results. The origin simply lies in the fact that the general and explicit \bar{U}_i -dependency in the scaling laws (5.15) for the velocity correlations result from two “statistical symmetries” \bar{T}'_s (2.17) and \bar{T}'_c (2.26) that violate the classical principle of cause and effect. That is, the \bar{U}_1 - as well as the \bar{U}_2 -dependency in the velocity correlations τ_{ij}^+ and τ_{ijk}^+ are simply *unphysical*. The negative results appear more strongly, of course, in the correlations involving the unphysical \bar{U}_1 -dependence.[†] The unphysical \bar{U}_2 -dependence, however, is less critical for the particular flow case considered here, since it is only a global constant, $\bar{U}_2 = v_0$. Worthwhile to note here is that the mismatch of τ_{11}^+ and τ_{112}^+ in Figure 5 is less severe for a higher transpiration rate than in Figure 4 for a lower one. The reason is that the unphysical \bar{U}_1 -dependence gets weaker for increasing transpiration rates, simply because the mean velocity field \bar{U}_1^+ itself is globally decaying for higher rates (see Figure 1).

Moreover, the key assumption in Avsarkisov *et al.* (2014) that an inviscid (Re_τ -independent) symmetry analysis is sufficient to capture the scaling behavior in the center of the channel, is not justified. Instead a strong sensitivity on Re_τ in the scaling laws (5.15) is observed, which, in comparison to Figure 4, is shown in Figure 6. This figure was generated under the assumption of Avsarkisov *et al.* (2014) that the Reynolds-number-independent scaling of the (non-normalized) higher-order moments (5.15) is correct: All involved parameters, once matched for a certain fixed Reynolds number Re_τ and transpiration rate v_0^+ , should then stay invariant as Re_τ changes. Of course, this assumed invariance should only hold for the *non*-normalized parameters as formulated in (5.15), and not for the u_τ -normalized ones, simply because the friction velocity u_τ itself changes when the Reynolds number Re_τ varies. Although this dependence $u_\tau \sim u_\tau(Re_\tau)$ is rather weak for a fixed transpiration rate v_0^+ and bulk velocity U_B^* as can be seen in Table 1,

[†]Note that we do not criticize the functional structure of the logarithmic scaling law of \bar{U}_1 itself, which can be more or less robustly matched to the DNS data in the channel center. We rather criticize its invariant Lie-group based derivation yielding this function with the aid of unphysical symmetries, and its consequent unnatural appearance in all higher order velocity correlations having a streamwise component. This criticism is all the more significant and pertinent as in Avsarkisov *et al.* (2014) the misleading impression is conveyed that the new logarithmic scaling law [Eq. (4.3)] for the channel center is based on a derivation from first principles. Yet, in this regard, it also should be clear that we do not criticize the method of Lie-groups itself, being a very useful mathematical tool indeed, when only applied to the right problems. However, in Avsarkisov *et al.* (2014) the method of Lie symmetry groups has been misapplied. The reason for this mistake was, and still is, not to recognize that every methodology in science has its limits, in particular the fact that also the theory of Lie-groups cannot analytically circumvent the closure problem of turbulence, even if the infinite hierarchy of statistical equations is formally considered. Because, instead of true symmetry transformations only the weaker form of equivalence transformation can be generated for such (unclosed) systems, for which, in a strict mathematical sense, the construction of invariant solutions is misleading and sometimes even ill-defined if no further external information is provided: For example, as to close the system of equations through some modelling assumptions, or, as in the specific case of homogeneous isotropic turbulence, where one has exclusive access to additional nonlocal invariants such as the Birkhoff-Saffman or the Loitsyansky integral, to yield more valuable results from such *equivalence* scaling groups, in particular the explicit values for the decay rates. For more details, we again refer to Frewer *et al.* (2014); Frewer (2015a,b) and the references therein.

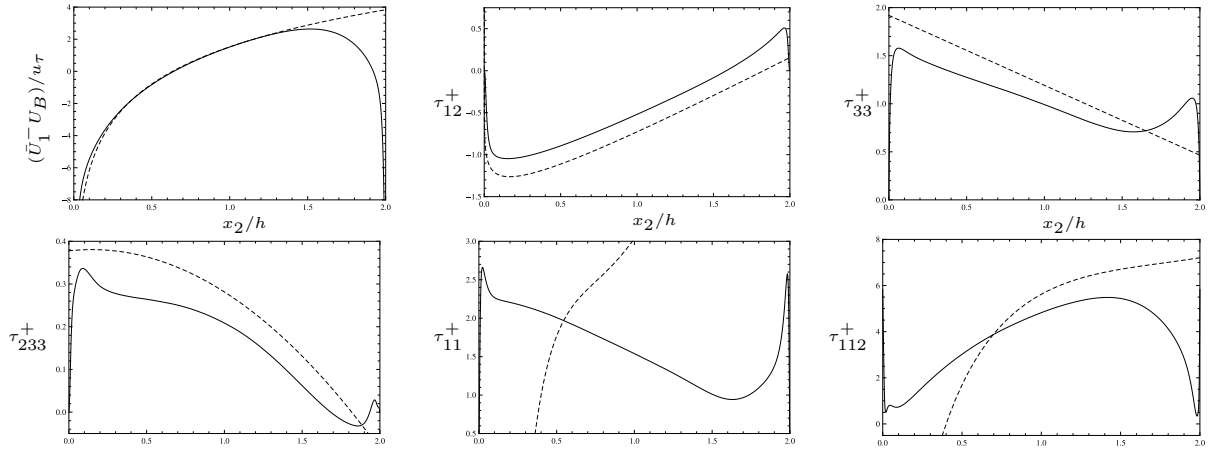


Figure 6: Sensitivity study on the Reynolds number Re_τ at fixed transpiration rate $v_0^+ = 0.05$. The solid lines display the DNS data for $Re_\tau = 850$; the dashed lines again the corresponding theoretically predicted (Re_τ -independent) scaling laws (5.15) as proposed by Avsarkisov *et al.* (2014) when coherently prolonged to higher-order moments. This figure is to be compared with Figure 4, having the same transpiration rate $v_0^+ = 0.05$ but at a lower Reynolds number $Re_\tau = 480$. Except for the mean velocity profile in deficit form, the strong sensitivity on Re_τ for all higher-order moments hence proves our conclusion in Section 3: The central assumption made in Avsarkisov *et al.* (2014), namely that the scaling of a turbulent channel flow with uniform wall-normal transpiration can be predicted by considering an *inviscid* ($\nu = 0$) symmetry analysis, i.e., by considering invariant solutions which, by construction, do not depend on Re_τ , is not justified at all. Important to note here is that this strong sensitivity only lies in the matching parameters of the scaling laws (5.15), and *not* in the DNS data itself. For more details on how the above figure was generated and its connection to Figure 4, see the main text.

this dependence, as was already discussed in Section 3, cannot be neglected, in particular not for any higher-order moments, where the relative change

$$\Delta_{\%} u_\tau^n = \frac{u_\tau^n(Re_\tau) - u_\tau^n(Re_\tau^*)}{u_\tau^n(Re_\tau^*)}, \quad (5.17)$$

in the normalization factor u_τ^n for a moment of order n becomes more pronounced for increased order, as can be seen in Figure 6. The Reynolds number Re_τ^* refers to some fixed reference value, which, in the considered case for $Re_\tau = 850$ in Figure 6, is given by $Re_\tau^* = 480$ (when compared to Figure 4). For example, for the given values $u_\tau|_{Re_\tau^*=480} \sim 0.0551$ and $u_\tau|_{Re_\tau=850} \sim 0.0501$, taken from Table 1 at the fixed transpiration rate $v_0^+ = 0.05$, the relative change in the normalization factor for the third order moment is already at $\Delta_{\%} u_\tau^3 \sim -25\%$; a change which definitely cannot be neglected anymore.

Now, while the matching to the DNS data in Figure 4 was performed in the u_τ -normalization for $Re_\tau^* = 480$, and since for its comparison to a higher Reynolds number in Figure 6 a corresponding u_τ -normalization for $Re_\tau = 850$ is needed, all “+”-parameters given in Table 2 have to be re-scaled by the ratio factor $\vartheta = u_\tau|_{Re_\tau^*=480}/u_\tau|_{Re_\tau=850} \sim 1.1011$ in order to shift the (assumed invariant) non-normalized parameters as formulated in (5.15) from $Re_\tau^* = 480$ to $Re_\tau = 850$. As mentioned before, although this factor ϑ is more or less close to one, it is not so anymore for the parametric values of any higher-order moments, where the change is significant. For example, for the normalized value \tilde{A}_{12}^+ of the second moment τ_{12}^+ , fitted in Figure 4 and listed in Table 2, the relative change is already about 20%:

$$\tilde{A}_{12}^+ \Big|_{Re_\tau^*=480} \sim -0.622 \xrightarrow{u_\tau^2|_{Re_\tau^*=480}} \tilde{A}_{12} \sim -0.002 \xrightarrow{1/u_\tau^2|_{Re_\tau^*=850}} \tilde{A}_{12}^+ \Big|_{Re_\tau=850} \sim -0.754. \quad (5.18)$$

It should be clear, that the scaling laws (5.15) in Figure 6 were not fitted to the DNS data, but the fact that they were obtained from the fitted results in Figure 4 by up-scaling the determined

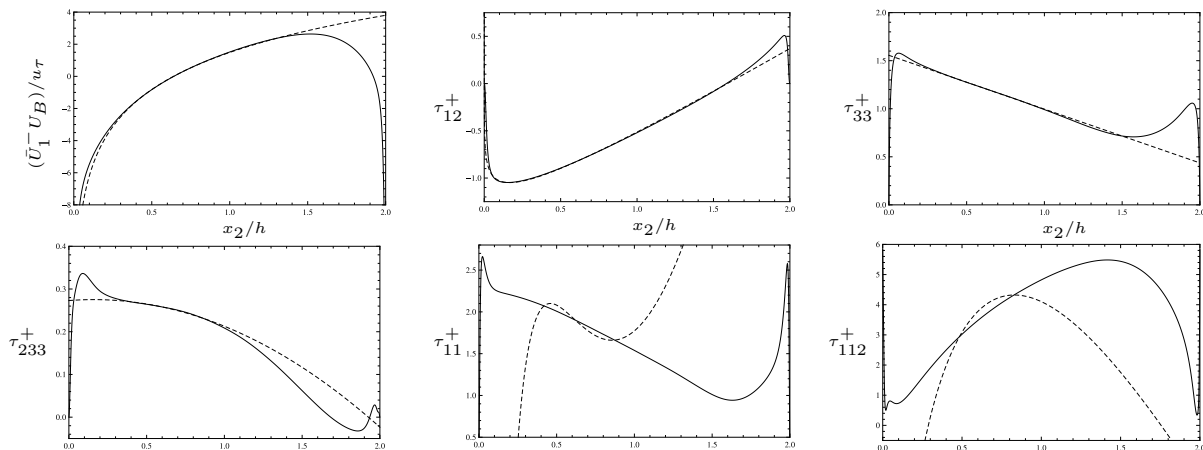


Figure 7: Matching of the theoretically predicted scaling laws (5.15) to the DNS data for $Re_\tau = 850$ and $v_0^+ = 0.05$. The DNS data is displayed by solid lines, the corresponding scaling laws by dashed lines. The associated (non-normalized) parameters for this best fit in each case can be taken from Table 3, where the matching region was chosen in the same range $0.50 \leq x_2/h \leq 1.25$ as for $Re_\tau = 480$ in Figure 4. For more details and a discussion on the fitting results obtained, see the main text.

parameters of Table 2 from $Re_\tau^* = 480$ to $Re_\tau = 850$ in using the procedure outlined in (5.18). Important to note here is that the up-scaling for the u_τ -normalized mean velocity field \bar{U}_1^+ , to be needed in the higher-order moments τ_{11}^+ , τ_{12}^+ and τ_{112}^+ , has been performed according to the (more or less correct) assumption of Avsarkisov *et al.* (2014) that the scaling law for the velocity field \bar{U}_1 in its deficit form (5.16) stays invariant for different Reynolds numbers at a fixed transpiration rate:

$$\frac{\bar{U}_1 - U_B^*}{u_\tau|_{Re_\tau^*=480}} = \frac{1}{\gamma} \ln(x_2/h) + \lambda = \frac{\bar{U}_1 - U_B^*}{u_\tau|_{Re_\tau=850}}, \quad (5.19)$$

which then can be solved to give the up-scaling relation for \bar{U}_1^+

$$\begin{aligned} \bar{U}_1^+|_{Re_\tau=850} &= \bar{U}_1^+|_{Re_\tau^*=480} - \frac{U_B^*}{u_\tau|_{Re_\tau^*=480}} + \frac{U_B^*}{u_\tau|_{Re_\tau=850}} \\ &= \left(\frac{1}{\gamma} \ln(x_2/h) + \lambda + \frac{U_B^*}{u_\tau|_{Re_\tau^*=480}} \right) - \frac{U_B^*}{u_\tau|_{Re_\tau^*=480}} + \frac{U_B^*}{u_\tau|_{Re_\tau=850}} \\ &= \frac{1}{\gamma} \ln(x_2/h) + \lambda + \frac{U_B^*}{u_\tau|_{Re_\tau=850}}. \end{aligned} \quad (5.20)$$

All these steps finally reveal the sensitivity of the invariant functions (5.15) on the Reynolds number Re_τ , as can be explicitly seen in Figure 6. Another option to study this sensitivity, is to re-fit again the scaling laws (5.15) to the DNS data for $Re_\tau = 850$, and to see how far the best-fitted values are off from the ones listed in Table 2 relative to the reference Reynolds-number $Re_\tau^* = 480$. As to be expected, the quality of the fit is similar to that of Figure 4, as can be seen in Figure 7, but it was achieved for different (non-normalized) parametric values which, as can be compared in Table 3, changed significantly, in particular the values for the two highest order moments τ_{112}^+ and τ_{233}^+ .

Anyhow, except for the mean velocity in deficit form, all higher-order moments show a strong sensitivity on the Reynolds number at fixed transpiration rate, thus clearly invalidating the inviscid assumption in Avsarkisov *et al.* (2014). It should be clear that this strong sensitivity

Re_τ	γ	λ	\tilde{A}_{12} [10^{-3}]	A_{33} [10^{-3}]	C_{33} [10^{-3}]	A_{233} [10^{-5}]	C_{233} [10^{-5}]	A_{11} [10^{-1}]	C_{11} [10^{-1}]	\tilde{A}_{112} [10^{-3}]	C_{112} [10^{-3}]
480	0.3	1.524	-1.888	4.807	-1.822	6.053	-1.710	-6.046	0.785	-4.744	0.478
850	0.3	1.491	-1.355	3.897	-1.402	4.398	-1.105	-5.437	0.873	-3.495	0.264

Table 3: Best-fitted (non-normalized) parameters of the theoretically predicted scaling laws (5.15) to the DNS data as shown in Figure 4 & 7 for two different Reynolds numbers $Re_\tau = 480$ and $Re_\tau = 850$, respectively, at $v_0^+ = 0.05$. In both cases, the parameter A_0^+ was fitted for τ_{11}^+ , and then applied in τ_{112}^+ : It takes the (non-normalized) value $A_0 = 0.761$ for $Re_\tau = 480$, and $A_0 = 0.723$ for $Re_\tau = 850$. Also, in both cases, the overall matching region was chosen in the range $0.50 \leq x_2/h \leq 1.25$. Except for A_0 and the parameters of the velocity profile (γ and λ), a strong Reynolds number dependence is observed throughout all scaling law parameters. Although the inviscid ($\nu = 0$) assumption in Avsarkisov *et al.* (2014) is more or less valid for the lowest order moment (the mean velocity), it is incorrect for all higher-order moments, in particular as the order of the moments increases, the Re_τ -dependence becomes more and more pronounced, e.g., for the third order parameter A_{233} we observe a relative change of nearly 30%.

only lies in the matching parameters of the Lie-group generated scaling laws (5.15), and *not* in the DNS data itself. In other words, these scaling laws cannot be robustly matched to the DNS data when assuming independence in one of its external system parameters.

Returning to the inconsistent symmetry analysis performed in Avsarkisov *et al.* (2014), in particular to the application of the unphysical scaling symmetry \bar{T}'_s (2.22), the mathematical proof in Frewer *et al.* (2014), Appendix D, clearly shows that independent of the particular flow configuration, the Lie-group based turbulent scaling laws for all higher order velocity correlations as derived in (5.15) are not consistent to the scaling of the mean velocity field itself. In other words, the proof in Frewer *et al.* (2014) shows that for the lowest correlation order $n = 1$ (defined as the mean velocity field) no contradiction exists, only as from $n = 2$ onwards the contradiction starts, i.e., while the mean velocity field can be robustly matched to the DNS data, it consistently fails for all higher order correlation functions and gets more pronounced the higher the correlation order n is.

Hence, to justify their new scaling law [Eq. (4.3)] in Avsarkisov *et al.* (2014) by saying that it “was successfully validated with DNS data for moderate transpiration rates” [p. 119] is based on a fallacy. The problem is that this “validation” in Avsarkisov *et al.* (2014) was only performed for the lowest order moment, which, of course, can always be matched to the DNS data since there are enough free parameters available to be fitted. But, as soon as any higher order correlations functions get fitted, not enough free parameters are available anymore and the curve-fitting procedure consistently fails in Avsarkisov *et al.* (2014), as shown in Figure 4 & 5.

Therefore, no true validation of the Lie-group-based scaling theory has been performed in Avsarkisov *et al.* (2014). For that also the theoretically predicted pressure-velocity correlations need to be validated against the DNS data to check in how far the best-fitted parameters are consistent with the parametric relations resulting from the underlying statistical transport equations (2.9)-(2.11) including *all* correlations, velocity as well as pressure. In particular, as the study of Avsarkisov *et al.* (2014) is based on the findings of Oberlack & Rosteck (2010) which specifically considers the infinite (unclosed) system of *all* multi-point correlation equations and which thus is designed and laid-out to be a “first principle” scaling theory for all higher order correlations (including velocity and pressure), special attention has to be devoted to the prediction value of all those correlation functions which go beyond the lowest or next to the lowest order. And exactly this has been investigated by us in the present study, however, yet only for the velocity correlation functions up to third order, but which already gives a different picture than the “validation” procedure in Avsarkisov *et al.* (2014) is trying to suggest. The same issue we also face in their subsequent publication Oberlack *et al.* (2015), which we will discuss next.

5.2. The viscous case ($\nu \neq 0$)

The viscous scaling theory to turbulent channel flow with constant wall-normal transpiration has not been studied in Avsarkisov *et al.* (2014). It only can be found in their subsequent publication Oberlack *et al.* (2015), where it is discussed in Sec. 6.2. For the same flow conditions as described in Section 2, the viscous transport equations corresponding to the inviscid ones (2.9)-(2.11) will have the extended form

$$\frac{\partial \bar{U}_2}{\partial x_2} = 0, \quad (5.21)$$

$$\frac{\partial \bar{U}_1 \bar{U}_2}{\partial x_2} + \frac{\partial \bar{P}}{\partial x_1} - \nu \frac{\partial^2 \bar{U}_1}{\partial x_2^2} = 0, \quad \frac{\partial \bar{U}_2 \bar{U}_2}{\partial x_2} + \frac{\partial \bar{P}}{\partial x_2} = 0, \quad \bar{U}_1 \bar{U}_3 = \bar{U}_2 \bar{U}_3 = 0, \quad (5.22)$$

$$\left. \begin{aligned} \frac{\partial \bar{U}_1 \bar{U}_2 \bar{U}_2}{\partial x_2} + \frac{\partial \bar{P}}{\partial x_1} \bar{U}_2 + \bar{U}_1 \frac{\partial \bar{P}}{\partial x_2} - \nu \bar{U}_1 \Delta \bar{U}_2 - \nu \bar{U}_2 \Delta \bar{U}_1 &= 0, \\ \frac{\partial \bar{U}_i \bar{U}_j \bar{U}_2}{\partial x_2} + \frac{\partial \bar{P}}{\partial x_i} \bar{U}_j + \bar{U}_i \frac{\partial \bar{P}}{\partial x_j} - \nu \bar{U}_i \Delta \bar{U}_j - \nu \bar{U}_j \Delta \bar{U}_i &= 0, \text{ for } i = j, \end{aligned} \right\} \quad (5.23)$$

where the second order viscous terms can also be equivalently written within their full-field form as

$$\nu \bar{U}_i \Delta \bar{U}_j + \nu \bar{U}_j \Delta \bar{U}_i = \nu \frac{\partial^2 \bar{U}_i \bar{U}_j}{\partial x_2^2} - 2\nu \frac{\partial \bar{U}_i}{\partial x_k} \frac{\partial \bar{U}_j}{\partial x_k}. \quad (5.24)$$

Decomposing this system into mean and fluctuating fields according to (2.8), we obtain the corresponding viscous Reynolds transport equations

$$\frac{\partial \bar{U}_2}{\partial x_2} = 0, \quad (5.25)$$

$$\bar{U}_2 \frac{\partial \bar{U}_1}{\partial x_2} + \frac{\partial \bar{P}}{\partial x_1} + \frac{\partial \tau_{12}}{\partial x_2} - \nu \frac{\partial^2 \bar{U}_1}{\partial x_2^2} = 0, \quad \frac{\partial \bar{P}}{\partial x_2} + \frac{\partial \tau_{22}}{\partial x_2} = 0, \quad \tau_{13} = \tau_{23} = 0, \quad (5.26)$$

$$\left. \begin{aligned} \bar{U}_2 \frac{\partial \tau_{12}}{\partial x_2} + \frac{\partial \tau_{122}}{\partial x_2} + \tau_{22} \frac{\partial \bar{U}_1}{\partial x_2} + \frac{\partial p}{\partial x_1} \bar{u}_2 + \bar{u}_1 \frac{\partial p}{\partial x_2} - \nu \frac{\partial^2 \tau_{12}}{\partial x_2^2} + \varepsilon_{12} &= 0, \\ \bar{U}_2 \frac{\partial \tau_{ij}}{\partial x_2} + \frac{\partial \tau_{ij2}}{\partial x_2} + \tau_{i2} \frac{\partial \bar{U}_j}{\partial x_2} + \tau_{j2} \frac{\partial \bar{U}_i}{\partial x_2} + \frac{\partial p}{\partial x_i} \bar{u}_j + \bar{u}_i \frac{\partial p}{\partial x_j} - \nu \frac{\partial^2 \tau_{ij}}{\partial x_2^2} + \varepsilon_{ij} &= 0, \text{ for } i = j, \end{aligned} \right\} \quad (5.27)$$

where ε_{ij} is the well-known dissipation tensor

$$\varepsilon_{ij} = 2\nu \frac{\partial \bar{u}_i}{\partial x_k} \frac{\partial \bar{u}_j}{\partial x_k}. \quad (5.28)$$

The set of symmetries admitted by (5.21)-(5.24) stays unchanged to the ones for the inviscid case used in the previous subsection, except for the two Euler scaling symmetries \bar{T}_1 (2.20) and \bar{T}_2 (2.21) which both break due the appearance of the viscous terms. Nevertheless, they recombine to give the classical Navier-Stokes scaling symmetry

$$\begin{aligned} \bar{T}_{\text{NS}} : \quad x_i^* &= e^{k_{\text{NS}}} x_i, \quad \bar{U}_i^* = e^{-k_{\text{NS}}} \bar{U}_i, \quad \bar{P}^* = e^{-2k_{\text{NS}}} \bar{P}, \quad \bar{U}_i \bar{U}_j^* = e^{-2k_{\text{NS}}} \bar{U}_i \bar{U}_j, \\ \bar{U}_i \bar{U}_j \bar{U}_k^* &= e^{-3k_{\text{NS}}} \bar{U}_i \bar{U}_j \bar{U}_k, \quad \bar{U}_i \frac{\partial \bar{P}}{\partial x_j}^* = e^{-4k_{\text{NS}}} \bar{U}_i \frac{\partial \bar{P}}{\partial x_j}, \\ \frac{\partial \bar{U}_i}{\partial x_k} \frac{\partial \bar{U}_j}{\partial x_k}^* &= e^{-4k_{\text{NS}}} \frac{\partial \bar{U}_i}{\partial x_k} \frac{\partial \bar{U}_j}{\partial x_k}. \end{aligned} \quad (5.29)$$

In Oberlack *et al.* (2015) another yet unmentioned symmetry is used which provokes to be analyzed in more detail. Due to the linearity of the MPC equations in their full-field representation, the governing system (5.21)-(5.24) admits the additional rather generic symmetry

$$\begin{aligned} \bar{T}'_+ : \quad x_i^* &= x_i, \quad \bar{U}_i^* = \bar{U}_i + F_i, \quad \bar{P}^* = \bar{P} + G, \quad \overline{U_i U_j}^* = \overline{U_i U_j} + F_{ij}, \\ \overline{U_i U_j U_k}^* &= \overline{U_i U_j U_k} + F_{ijk}, \quad \overline{U_i \frac{\partial P}{\partial x_j}}^* = \overline{U_i \frac{\partial P}{\partial x_j}} + G_{ij}, \\ \frac{\partial \bar{U}_i}{\partial x_k} \frac{\partial \bar{U}_j}{\partial x_k}^* &= \frac{\partial \bar{U}_i}{\partial x_k} \frac{\partial \bar{U}_j}{\partial x_k} + L_{ij}, \end{aligned} \quad (5.30)$$

where the functions F_i , F_{ij} , F_{ijk} , G , $G_{ij} \neq G_{ji}$ and L_{ij} are any particular solutions of the governing system of equations (5.21)-(5.24), i.e., where these functions satisfy again the equations

$$\frac{\partial F_2}{\partial x_2} = 0, \quad (5.31)$$

$$\frac{\partial F_{12}}{\partial x_2} + \frac{\partial G}{\partial x_1} - \nu \frac{\partial^2 F_1}{\partial x_2^2} = 0, \quad \frac{\partial F_{22}}{\partial x_2} + \frac{\partial G}{\partial x_2} = 0, \quad F_{13} = F_{23} = 0, \quad (5.32)$$

$$\left. \begin{aligned} \frac{\partial F_{122}}{\partial x_2} + G_{12} + G_{21} - \nu \frac{\partial^2 F_{12}}{\partial x_2^2} + 2\nu L_{12} &= 0, \\ \frac{\partial F_{ij2}}{\partial x_2} + G_{ij} + G_{ji} - \nu \frac{\partial^2 F_{ij}}{\partial x_2^2} + 2\nu L_{ij} &= 0, \text{ for } i = j. \end{aligned} \right\} \quad (5.33)$$

This symmetry just reflects the superposition property which is featured by all (homogeneous) linear differential equations. However, this symmetry is of no value, because, as correctly already noted in Oberlack & Rostek (2010), it ‘‘cannot directly be adopted for the practical derivation of group invariant solutions’’ [p.463]. The simple reason is that the system of equations (5.31)-(5.33) is unclosed and no analytical solution is known yet which is consistent up to all higher orders in its infinite hierarchy, otherwise one would have found a solution to the still unsolved closure problem of turbulence. Any guessed solution, which only satisfies the system (5.31)-(5.33) up to a fixed order $n = n_0$ in its infinite hierarchy, is of no value if we cannot guarantee that (i) this solution is also consistent for all higher orders $n > n_0$, and (ii) that it also represents a physical solution which is consistent to the DNS data; because, for such unclosed systems, infinitely many different and independent mathematical solutions can be generated which all in the end are *not* reflected in the DNS data (Frewer *et al.*, 2014; Frewer, 2015a,b).

Despite their concern in Oberlack & Rostek (2010) that the superposition symmetry due to the closure problem cannot be exploited, it nevertheless was used in Oberlack *et al.* (2015) to generate invariant solutions. Therein the superposition symmetry \bar{T}'_+ (5.30) shows its existence through the arbitrarily chosen symmetries $Z_{z_{ij}}$ in [Eq.(353)], where some of the functional translations in (5.30) were arbitrarily fixed as linear functions (in the one-point limit $\mathbf{r} \rightarrow \mathbf{0}$):

$$\left. \begin{aligned} F_i &= G_{ij} = L_{ij} = F_{ijk} = 0, \quad G = -k_{z_{12}}x_1 - 2k_{z_{22}}x_2, \\ F_{11} &= 2k_{z_{11}}x_2, \quad F_{12} = k_{z_{12}}x_2, \quad F_{22} = 2k_{z_{22}}x_2, \quad F_{33} = 2k_{z_{33}}x_2. \end{aligned} \right\} \quad (5.34)$$

The motivation to choose this particular set of (linear) functions (5.34) and not any other set of functions that may also solve the system (5.31)-(5.33), is not clear. However, if the motivation was such as to only gain a better matching of the invariant functions to the DNS data, then the procedure proposed in Oberlack *et al.* (2015) has nothing to do with a theoretical prediction or forecasting of turbulent scaling laws as claimed therein. Because, such an approach would then just be based on a trial and error procedure which incrementally improves the prediction of turbulent scaling only *a posteriori*, and not *a priori*, as required for a true theoretical and ‘‘first principle’’ ansatz. In other words, since we don’t see in Oberlack *et al.* (2015) any clear motivation *a priori* for a linear solution ansatz of the functional translational symmetries $Z_{z_{ij}}$ [Eq.(353)], it seems that they were chosen *a posteriori* to only enhance the matching to the

DNS data. But, as already said, such an approach is not in the sense of the inventor to forecast turbulent scaling laws from a “first principle” theory which is “fully algorithmic” and where “no intuition is needed” (Oberlack, 2001, p. 321). Hence, through the use of the superposition principle \bar{T}'_+ (5.30) in an unclosed system (5.21)-(5.24), the Lie-group symmetry approach in Oberlack *et al.* (2015) degenerates down to a *non*-predictive incremental trial-and-error method.

But, as already discussed in the conclusion of the previous subsection, no matter how great the effort to incrementally improve the predictive ability of Lie-group generated invariant solutions for turbulent scaling, the methodological approach itself, as initially proposed in Oberlack & Rosteck (2010) and last applied in Oberlack *et al.* (2015), will always be inconsistent in that a comparison to DNS data will always fail when considering correlation orders higher than the well-matched threshold level of a lower correlation order. The simple reason is that the analysis is permanently set up by two unphysical “statistical symmetries” \bar{T}'_s (2.22) and \bar{T}'_c (2.25) that perpetually violate the classical principle of cause and effect. The only way thus to obtain an overall *consistent* symmetry analysis, is to discard all unphysical symmetries (Frewer *et al.*, 2014, 2015; Frewer, 2015c; Frewer *et al.*, 2016).

When combining all symmetry groups (2.22)-(2.25), (5.29) and (5.30) with (5.34), we now obtain, instead of the inviscid invariant surface condition (5.1), the viscous condition

$$\begin{aligned}
\frac{dx_1}{k_{\text{NS}}x_1 + k_{x_1}} &= \frac{dx_2}{k_{\text{NS}}x_2 + k_{x_2}} = \frac{d\bar{U}_i}{(-k_{\text{NS}} + k_s)\bar{U}_i + \omega_i + \kappa_i + c_i} = \frac{d\bar{P}}{(-2k_{\text{NS}} + k_s)\bar{P} + \omega^p + \kappa^p + d} \\
&= \frac{d(\partial_i\bar{P})}{(-3k_{\text{NS}} + k_s)\partial_i\bar{P} + \omega_i^p + \kappa_i^p} \\
&= \frac{d\bar{U}_i\bar{U}_j}{(-2k_{\text{NS}} + k_s)\bar{U}_i\bar{U}_j + \omega_{ij} + \kappa_{ij} + c_{ij}} \\
&= \frac{d\bar{U}_i\bar{U}_j\bar{U}_k}{(-3k_{\text{NS}} + k_s)\bar{U}_i\bar{U}_j\bar{U}_k + \omega_{ijk} + \kappa_{ijk} + c_{ijk}} \\
&= \frac{d\bar{U}_i\partial_j\bar{P}}{(-4k_{\text{NS}} + k_s)\bar{U}_i\partial_j\bar{P} + \omega_{ij}^p + \kappa_{ij}^p} \\
&= \frac{d\partial_k\bar{U}_i \cdot \partial_k\bar{U}_j}{(-4k_{\text{NS}} + k_s)\partial_k\bar{U}_i \cdot \partial_k\bar{U}_j + \omega_{ij}^\nu + \kappa_{ij}^\nu}, \tag{5.35}
\end{aligned}$$

where the functional ω -extensions, resulting from the linear superposition symmetry \bar{T}'_+ (5.30), are given as

$$\left. \begin{aligned}
\omega_i &= 0, \\
\omega_{ij} &= 2k_{z11}x_2\delta_{1i}\delta_{1j} + 2k_{z22}x_2\delta_{2i}\delta_{2j} + 2k_{z33}x_2\delta_{3i}\delta_{3j} + k_{z12}x_2(\delta_{1i}\delta_{2j} + \delta_{1j}\delta_{2i}), \\
\omega_{ijk} &= 0, \quad \omega^p = -k_{z12}x_1 - 2k_{z22}x_2, \quad \omega_i^p = -k_{z12}\delta_{1i} - 2k_{z22}\delta_{2i}, \\
\omega_{ij}^p &= 0, \quad \omega_{ij}^\nu = 0,
\end{aligned} \right\} \tag{5.36}$$

and the functional κ -extensions, resulting again from the translation symmetry \bar{T}'_{U_1} (2.24), as

$$\left. \begin{aligned}
\kappa_i &= k_{\bar{U}_1}\delta_{1i}, \quad \kappa_{ij} = \kappa_i\bar{U}_j + \kappa_j\bar{U}_i, \\
\kappa_{ijk} &= \kappa_{ij}\bar{U}_k + \kappa_{ik}\bar{U}_j + \kappa_{jk}\bar{U}_i \\
&\quad + \kappa_i(\bar{U}_j\bar{U}_k - 2\bar{U}_j\bar{U}_k) + \kappa_j(\bar{U}_i\bar{U}_k - 2\bar{U}_i\bar{U}_k) + \kappa_k(\bar{U}_i\bar{U}_j - 2\bar{U}_i\bar{U}_j), \\
\kappa^p &= 0, \quad \kappa_i^p = 0, \quad \kappa_{ij}^p = \kappa_i\frac{\partial\bar{P}}{\partial x_j}, \quad \kappa_{ij}^\nu = 0.
\end{aligned} \right\} \tag{5.37}$$

When comparing the full-field invariant surface condition (5.35) with the correspondingly given Reynolds-decomposed condition [Eq. (354)] in Oberlack *et al.* (2015), one can recognize that in the one-point limit ($\mathbf{r} \rightarrow \mathbf{0}$) both conditions are indeed equivalent, except on three points:

(i) Instead of the two independent translation symmetries $\bar{T}_{\bar{U}_1}$ (2.19) and \bar{T}'_c (2.26), the equivalent set of transformations $\bar{T}_{\bar{U}_1}$ and $\bar{T}_{\text{tr},1} := \bar{T}'_c|_{c_1=k_{\text{tr},1}} \circ \bar{T}_{\bar{U}_1}|_{k_{\bar{U}_1}=-k_{\text{tr},1}}$ has been used in Oberlack *et al.* (2015). For more details see also Rosteck (2014) [pp. 228-229].

(ii) The invariant (symmetry breaking) constraint $\bar{U}_2^* = \bar{U}_2$ of a constant wall-normal transpiration velocity $\bar{U}_2 = v_0$ (denoted in Oberlack *et al.* (2015) as U_T) has already been directly implemented in both scaling symmetries \bar{T}'_s (2.22) and \bar{T}_{NS} (5.29), namely by transferring these full-field symmetries back to their corresponding Reynolds-decomposed form under the separate conditions $k_s \neq 0$ and $k_{\text{NS}} \neq 0$. Such a procedure, however, is based on a fallacy, as we will show further below, because consistency reveals that k_s and k_{NS} each must be zero, i.e., when imposing the constraint $\bar{U}_2^* = \bar{U}_2$, the symmetry breaking cannot be circumvented, no matter which *modus operandi* is applied.

(iii) The infinitesimal generator for R_{12} in [Eq. (354)] in Oberlack *et al.* (2015) contains two misprints: The term “ $-k_{z,2}x_2U_T$ ” has to be deleted, since a parameter such as $k_{z,2}$ does not exist, neither in the considered symmetries nor in the derived invariant solutions [Eq. (357)] and [Eq. (363)]. Similar for the misprinted parameter “ $k_{\text{sc},\text{tr}2}$ ”, which should be replaced by k_{NS} . Both misprints also appear in Rosteck (2014) [p. 228].

As also already outlined in the previous subsection, we recall again that before invariant solutions get determined from (5.35), we first have to ensure the invariance of two enclosed system constraints: That of a mean constant wall-normal velocity $\bar{U}_2 = v_0$, or, equivalently $d\bar{U}_2 = 0$, and that of a mean constant streamwise pressure gradient $\partial\bar{P}/\partial x_1 = -K$, or, equivalently $d(\partial_1\bar{P}) = 0$. Implementing these into (5.35) will then collectively result into the following symmetry breaking constraints

$$-k_{\text{NS}} + k_s = 0, \quad c_2 = 0, \quad \text{and} \quad -3k_{\text{NS}} + k_s = 0, \quad \omega_1^p = 0, \quad (5.38)$$

which leads us to the equivalent restrictions

$$k_{\text{NS}} = 0, \quad k_s = 0, \quad c_2 = 0, \quad k_{z12} = 0. \quad (5.39)$$

Consequently, the only invariant structure that can be derived for the mean velocity profile \bar{U}_1 from (5.35) is that of a linear function

$$\bar{U}_1(x_2) = \alpha \cdot x_2 + \beta, \quad (5.40)$$

which, of course, does not constitute a reasonable scaling law (where $\alpha = (k_{\bar{U}_1} + c_1)/k_{x_2}$ and β some arbitrary integration constant). Hence, in contrast to the inviscid symmetry analysis performed in the previous subsection which only fails at a higher-order moment, the current viscous analysis already fails at the lowest-order moment \bar{U}_1 . The reason is that the viscous analysis misses out one scaling symmetry: Instead of three inviscid scaling symmetries, \bar{T}_1 (2.20), \bar{T}_2 (2.21) and \bar{T}'_s (2.22), we only face two possible scaling symmetries for the viscous case, namely \bar{T}_{NS} (5.29) and again \bar{T}'_s (2.22), which turns out to be crucial when at least two independent symmetry breaking constraints are imposed, as can be seen in (5.38), or (5.39), where both scaling symmetries then get broken.

Although due to the symmetry breaking (5.39) no logarithmic or algebraic scaling for the mean velocity profile \bar{U}_1 can be derived, the corresponding analysis carried out in Oberlack *et al.* (2015), however, nevertheless succeeded to do so. The mistake lies in the fallacy already pointed out in (ii) above. To comprehend the mistake that has been done in Oberlack *et al.* (2015), let us repeat their line of reasoning by first looking at the scaling symmetry \bar{T}_{NS} (5.29) in how the invariant (symmetry breaking) constraint $\bar{U}_2^* = \bar{U}_2$ of a constant wall-normal transpiration velocity $\bar{U}_2 = U_T$ has been implemented under the condition of a non-zero group parameter

$k_{\text{NS}} \neq 0$ associated to that symmetry. The details can also be found in Rosteck (2014) [p. 229]. Although the same line of reasoning has also been used for the second scaling symmetry \bar{T}'_s (2.22), we will discuss it separately, due to being a special symmetry.

The starting point are the *full-field* statistical transport equations (5.21)-(5.24), where we explicitly insert the constraint of a constant wall-normal transpiration velocity $\overline{U_2}(x_2) = U_T$:

$$\frac{\partial \overline{U_1 U_2}}{\partial x_2} + \frac{\partial \bar{P}}{\partial x_1} - \nu \frac{\partial^2 \overline{U_1}}{\partial x_2^2} = 0, \quad \frac{\partial \overline{U_2 U_2}}{\partial x_2} + \frac{\partial \bar{P}}{\partial x_2} = 0, \quad \overline{U_1 U_3} = \overline{U_2 U_3} = 0, \quad (5.41)$$

$$\left. \begin{aligned} \frac{\partial \overline{U_1 U_2 U_2}}{\partial x_2} + \frac{\partial \bar{P}}{\partial x_1} U_2 + U_1 \frac{\partial \bar{P}}{\partial x_2} - \nu \frac{\partial^2 \overline{U_1 U_2}}{\partial x_2^2} + 2\nu \frac{\partial \overline{U_1}}{\partial x_k} \frac{\partial \overline{U_2}}{\partial x_k} &= 0, \\ \frac{\partial \overline{U_i U_j U_2}}{\partial x_2} + \frac{\partial \bar{P}}{\partial x_i} U_j + U_i \frac{\partial \bar{P}}{\partial x_j} - \nu \frac{\partial^2 \overline{U_i U_j}}{\partial x_2^2} + 2\nu \frac{\partial \overline{U_i}}{\partial x_k} \frac{\partial \overline{U_j}}{\partial x_k} &= 0, \text{ for } i = j. \end{aligned} \right\} \quad (5.42)$$

As a result, these equations do not depend anymore on the mean wall-normal velocity $\overline{U_2}$, and this observation is true for all orders in the infinite hierarchy of equations. Hence, based on the scaling symmetry \bar{T}_{NS} (5.29) for the initial system (5.21)-(5.24), we now may consider a modified symmetry \bar{Q}_{NS} that already inherently respects the required invariant constraint $\overline{U_2}^* = \overline{U_2} = U_T$:

$$\begin{aligned} \bar{Q}_{\text{NS}} : \quad x_i^* &= e^{q_{\text{NS}}} x_i, \quad \overline{U_1}^* = e^{-q_{\text{NS}}} \overline{U_1}, \quad \overline{U_2}^* = \overline{U_2}, \quad \bar{P}^* = e^{-2q_{\text{NS}}} \bar{P}, \quad \overline{U_i U_j}^* = e^{-2q_{\text{NS}}} \overline{U_i U_j}, \\ \overline{U_i U_j U_k}^* &= e^{-3q_{\text{NS}}} \overline{U_i U_j U_k}, \quad \overline{U_i \frac{\partial \bar{P}}{\partial x_j}}^* = e^{-4q_{\text{NS}}} \overline{U_i \frac{\partial \bar{P}}{\partial x_j}}, \\ \overline{\frac{\partial U_i}{\partial x_k} \frac{\partial U_j}{\partial x_k}}^* &= e^{-4q_{\text{NS}}} \overline{\frac{\partial U_i}{\partial x_k} \frac{\partial U_j}{\partial x_k}}. \end{aligned} \quad (5.43)$$

Indeed, transformation (5.43) is admitted as a symmetry by the equations (5.41)-(5.42) as can be readily verified. However, important to note here is that \bar{Q}_{NS} (5.43) is a different scaling symmetry than the initially considered \bar{T}_{NS} (5.29), i.e., the latter symmetry cannot be reduced to the former one. With \bar{Q}_{NS} (5.43) we obtained a symmetry that automatically obeys the invariant constraint $\overline{U_2}^* = \overline{U_2} = U_T$ without breaking the group parameter q_{NS} down to zero; a result impossible to achieve with the initial scaling symmetry \bar{T}_{NS} (5.29). Hence, when generating invariant solutions under the constraint $\overline{U_2}^* = \overline{U_2} = U_T$, the Navier-Stokes scaling symmetry \bar{T}_{NS} (5.29) has to be replaced by its appropriate but non-linked modification \bar{Q}_{NS} (5.43).

In its equivalent Reynolds-decomposed form, the symmetry \bar{Q}_{NS} (5.43) reads (Rosteck, 2014; Oberlack *et al.*, 2015):

$$\begin{aligned} \bar{Q}_{\text{NS}} : \quad x_i^* &= e^{q_{\text{NS}}} x_i, \quad \bar{U}_i^* = e^{-q_{\text{NS}}} \bar{U}_1 \delta_{1i} + U_T \delta_{2i}, \quad \bar{P}^* = e^{-2q_{\text{NS}}} \bar{P}, \\ \tau_{ij}^* &= e^{-2q_{\text{NS}}} \tau_{ij} + e^{-2q_{\text{NS}}} \bar{U}_i \bar{U}_j - \bar{U}_i^* \bar{U}_j^*, \\ &= e^{-2q_{\text{NS}}} \tau_{ij} + \left(e^{-2q_{\text{NS}}} - e^{-q_{\text{NS}}} \right) \bar{U}_1 U_T \left(\delta_{1i} \delta_{2j} + \delta_{1j} \delta_{2i} \right) + \left(e^{-2q_{\text{NS}}} - 1 \right) U_T^2 \delta_{2i} \delta_{2j}, \\ \tau_{ijk}^* &= e^{-3q_{\text{NS}}} \tau_{ijk} + e^{-3q_{\text{NS}}} \left(\bar{U}_i \bar{U}_j \bar{U}_k + \bar{U}_i \tau_{jk} + \bar{U}_j \tau_{ik} + \bar{U}_k \tau_{ij} \right) \\ &\quad - \bar{U}_i^* \bar{U}_j^* \bar{U}_k^* - \bar{U}_i^* \tau_{jk}^* - \bar{U}_j^* \tau_{ik}^* - \bar{U}_k^* \tau_{ij}^*, \\ \overline{u_i \frac{\partial p}{\partial x_j}}^* &= e^{-4q_{\text{NS}}} \overline{u_i \frac{\partial p}{\partial x_j}} + e^{-4q_{\text{NS}}} \bar{U}_i \frac{\partial \bar{P}}{\partial x_j} - \bar{U}_i^* \frac{\partial \bar{P}^*}{\partial x_j^*}, \\ \varepsilon_{ij}^* &= e^{-4q_{\text{NS}}} \varepsilon_{ij} + e^{-4q_{\text{NS}}} 2\nu \frac{\partial \bar{U}_i}{\partial x_2} \frac{\partial \bar{U}_j}{\partial x_2} - 2\nu \frac{\partial \bar{U}_i^*}{\partial x_2^*} \frac{\partial \bar{U}_j^*}{\partial x_2^*}, \end{aligned} \quad (5.44)$$

which indeed is a symmetry of the corresponding Reynolds-decomposed transport equations (5.25)-(5.28) for $\bar{U}_2 = U_T$:

$$U_T \frac{\partial \bar{U}_1}{\partial x_2} + \frac{\partial \bar{P}}{\partial x_1} + \frac{\partial \tau_{12}}{\partial x_2} - \nu \frac{\partial^2 \bar{U}_1}{\partial x_2^2} = 0, \quad \frac{\partial \bar{P}}{\partial x_2} + \frac{\partial \tau_{22}}{\partial x_2} = 0, \quad \tau_{13} = \tau_{23} = 0, \quad (5.45)$$

$$\left. \begin{aligned} U_T \frac{\partial \tau_{12}}{\partial x_2} + \frac{\partial \tau_{122}}{\partial x_2} + \tau_{22} \frac{\partial \bar{U}_1}{\partial x_2} + \frac{\partial p}{\partial x_1} u_2 + u_1 \frac{\partial p}{\partial x_2} - \nu \frac{\partial^2 \tau_{12}}{\partial x_2^2} + \varepsilon_{12} &= 0, \\ U_T \frac{\partial \tau_{ij}}{\partial x_2} + \frac{\partial \tau_{ij2}}{\partial x_2} + \tau_{i2} \frac{\partial \bar{U}_j}{\partial x_2} + \tau_{j2} \frac{\partial \bar{U}_i}{\partial x_2} + \frac{\partial p}{\partial x_i} u_j + u_i \frac{\partial p}{\partial x_j} - \nu \frac{\partial^2 \tau_{ij}}{\partial x_2^2} + \varepsilon_{ij} &= 0, \text{ for } i = j. \end{aligned} \right\} (5.46)$$

Although \bar{Q}_{NS} (5.44) is mathematically correctly admitted as a symmetry transformation by the infinite and unclosed system of statistical equations (5.45)-(5.46), it nevertheless has to be checked whether this symmetry is also consistent with the underlying deterministic Navier-Stokes equations, in particular because \bar{Q}_{NS} (5.44) acts as a purely statistical symmetry which is not reflected in the original deterministic equations. Hence, it is necessary to check whether this symmetry violates the principle of cause and effect. As explained and discussed in Frewer *et al.* (2014, 2015, 2016), no violation of causality occurs if at least one (invertible) deterministic transformation \mathcal{Q}_{NS} of the Navier-Stokes equations can be found such that then the symmetry \bar{Q}_{NS} (5.44) is induced on the statistical level, i.e., $\langle \mathcal{Q}_{\text{NS}} \rangle = \bar{Q}_{\text{NS}}$, where $\langle \cdot \rangle$ denotes any statistical averaging operator. Important to note here is that the deterministic cause \mathcal{Q}_{NS} itself need *not* to be symmetry in order to induce the statistical symmetry \bar{Q}_{NS} as an effect.

The aim is to find at least one (invertible) deterministic transformation \mathcal{Q}_{NS} (which itself need not to be a symmetry) of the Navier-Stokes equations

$$\begin{aligned} \mathcal{Q}_{\text{NS}} : \quad t^* &= t^*(t, x_i, \bar{U}_i, \bar{P}, u_i, p), \quad x_i^* = e^{q_{\text{NS}}} x_i, \quad \bar{U}_i^* = e^{-q_{\text{NS}}} \bar{U}_1 \delta_{1i} + \bar{U}_2 \delta_{2i}, \quad \bar{U}_3^* = \bar{U}_3 = 0, \\ u_i^* &= u_i^*(t, x_i, \bar{U}_i, \bar{P}, u_i, p), \quad \bar{P}^* = e^{-2q_{\text{NS}}} \bar{P}, \quad p^* = p^*(t, x_i, \bar{U}_i, \bar{P}, u_i, p), \end{aligned} \quad (5.47)$$

such that it induces the statistical symmetry \bar{Q}_{NS} (5.44), i.e., such that $\langle \mathcal{Q}_{\text{NS}} \rangle = \bar{Q}_{\text{NS}}$. We will restrict the analysis only to point transformations, where the transformations for the fluctuations u_i^* and p^* , as well as for the time t^* , are unknown transformations that need to be determined. We start off with the symmetry transformation of τ_{33}^* , for which, according to (5.44), the transformed fluctuation u_3^* has to be the deterministic cause for the statistical symmetry-effect

$$\langle u_3^{*2} \rangle = e^{-2q_{\text{NS}}} \langle u_3^2 \rangle, \quad (5.48)$$

which can only be satisfied if u_3^* transforms as

$$u_3^* = e^{-q_{\text{NS}}} u_3. \quad (5.49)$$

Then by considering the symmetry transformation of τ_{23}^* (5.44)

$$\langle u_2^* u_3^* \rangle = e^{-2q_{\text{NS}}} \langle u_2 u_3 \rangle, \quad (5.50)$$

this effect, when incorporating the previous result (5.49), can only be caused by

$$u_2^* = e^{-q_{\text{NS}}} u_2, \quad (5.51)$$

but which then is inconsistent to the effect observed by τ_{22}^* (5.44)

$$\langle u_2^{*2} \rangle = e^{-2q_{\text{NS}}} \langle u_2^2 \rangle + (e^{-2q_{\text{NS}}} - 1) U_T^2. \quad (5.52)$$

As can be readily seen, a consistent transformation can only be achieved if

$$(e^{-2q_{\text{NS}}} - 1) U_T^2 = 0, \quad (5.53)$$

and since $U_T \neq 0$, we thus yield the result

$$q_{\text{NS}} = 0. \quad (5.54)$$

Hence, for $q_{\text{NS}} \neq 0$, the statistical symmetry \bar{Q}_{NS} (5.44) is violating the classical principle of cause and effect, since obviously no deterministic cause \mathcal{Q}_{NS} (5.47) can be found that statistically induces this symmetry-effect \bar{Q}_{NS} (5.44). The statistical symmetry \bar{Q}_{NS} (5.44) is thus inconsistent to its underlying deterministic theory, and can only be restored if $q_{\text{NS}} = 0$, i.e. if the symmetry gets broken.

The same line of reasoning also applies to the second scaling symmetry \bar{T}'_s (2.22). Based on this symmetry for the initial system (5.21)-(5.24), the analysis in Oberlack *et al.* (2015) considers again a modified symmetry \bar{Q}_s such that it already inherently respects again the required invariant constraint $\bar{U}_2^* = \bar{U}_2 = U_T$:

$$\begin{aligned} \bar{Q}_s : \quad x_i^* &= x_i, \quad \bar{U}_1^* = e^{q_s} \bar{U}_1, \quad \bar{U}_2^* = \bar{U}_2, \quad \bar{P}^* = e^{q_s} \bar{P}, \quad \overline{U_i U_j}^* = e^{q_s} \overline{U_i U_j}, \\ \overline{U_i U_j U_k}^* &= e^{q_s} \overline{U_i U_j U_k}, \quad \overline{U_i \frac{\partial P}{\partial x_j}}^* = e^{q_s} \overline{U_i \frac{\partial P}{\partial x_j}}, \\ \overline{\frac{\partial U_i}{\partial x_k} \frac{\partial U_j}{\partial x_k}}^* &= e^{q_s} \overline{\frac{\partial U_i}{\partial x_k} \frac{\partial U_j}{\partial x_k}}, \end{aligned} \quad (5.55)$$

which indeed is a symmetry of the considered full-field system (5.41)-(5.42). In its equivalent Reynolds-decomposed form, this symmetry reads (Rosteck, 2014; Oberlack *et al.*, 2015):

$$\begin{aligned} \bar{Q}_s : \quad x_i^* &= x_i, \quad \bar{U}_i^* = e^{q_s} \bar{U}_i \delta_{1i} + U_T \delta_{2i}, \quad \bar{P}^* = e^{q_s} \bar{P}, \\ \tau_{ij}^* &= e^{q_s} \tau_{ij} + e^{q_s} \bar{U}_i \bar{U}_j - \bar{U}_i^* \bar{U}_j^*, \\ &= e^{q_s} \tau_{ij} + (e^{q_s} - e^{2q_s}) \bar{U}_1^2 \delta_{1i} \delta_{1j} + (e^{q_s} - 1) U_T^2 \delta_{2i} \delta_{2j}, \\ \tau_{ijk}^* &= e^{q_s} \tau_{ijk} + e^{q_s} (\bar{U}_i \bar{U}_j \bar{U}_k + \bar{U}_i \tau_{jk} + \bar{U}_j \tau_{ik} + \bar{U}_k \tau_{ij}) \\ &\quad - \bar{U}_i^* \bar{U}_j^* \bar{U}_k^* - \bar{U}_i^* \tau_{jk}^* - \bar{U}_j^* \tau_{ik}^* - \bar{U}_k^* \tau_{ij}^*, \\ \overline{u_i \frac{\partial p}{\partial x_j}}^* &= e^{q_s} \overline{u_i \frac{\partial p}{\partial x_j}} + e^{q_s} \bar{U}_i \frac{\partial \bar{P}}{\partial x_j} - \bar{U}_i^* \frac{\partial \bar{P}^*}{\partial x_j^*}, \\ \varepsilon_{ij}^* &= e^{q_s} \varepsilon_{ij} + e^{q_s} 2\nu \frac{\partial \bar{U}_i}{\partial x_2} \frac{\partial \bar{U}_j}{\partial x_2} - 2\nu \frac{\partial \bar{U}_i^*}{\partial x_2^*} \frac{\partial \bar{U}_j^*}{\partial x_2^*}, \end{aligned} \quad (5.56)$$

which indeed is also a symmetry of the corresponding Reynolds-decomposed transport equations (5.45)-(5.46). However, as in the previous case for \bar{Q}_{NS} (5.44), although the second scaling transformation \bar{Q}_s (5.56) is also mathematically correctly admitted as a symmetry by its statistical equations, it nevertheless is inconsistent to its underlying deterministic description, too, since, also in this case, no deterministic cause

$$\begin{aligned} \mathcal{Q}_s : \quad t^* &= t^*(t, x_i, \bar{U}_i, \bar{P}, u_i, p), \quad x_i^* = x_i, \quad \bar{U}_i^* = e^{q_s} \bar{U}_i \delta_{1i} + \bar{U}_2 \delta_{2i}, \quad \bar{U}_3^* = \bar{U}_3 = 0, \\ u_i^* &= u_i^*(t, x_i, \bar{U}_i, \bar{P}, u_i, p), \quad \bar{P}^* = e^{q_s} \bar{P}, \quad p^* = p^*(t, x_i, \bar{U}_i, \bar{P}, u_i, p), \end{aligned} \quad (5.57)$$

can be found such that on its statistical level the symmetry \bar{Q}_s (5.56) can be observed, that is, such that $\langle \mathcal{Q}_s \rangle = \bar{Q}_s$, where the deterministic cause \mathcal{Q}_s (5.57), of course, need not to be symmetry of the Navier-Stokes equations itself, in order to induce a symmetry as a statistical effect. Following the same procedure as outlined in (5.48)-(5.53) for \bar{Q}_{NS} (5.44), one again readily sees that the statistical scaling symmetry \bar{Q}_s (5.56) only can be made consistent to its

underlying deterministic description if $q_s = 0$. Hence, as in the full-field representation, where we obtained the symmetry-breaking result (5.39)

$$k_{\text{NS}} = 0, \quad k_s = 0, \quad (5.58)$$

for the two scaling symmetries \bar{T}_{NS} (5.29) and \bar{T}'_s (2.22), we thus also obtain the equivalent result in the Reynolds-decomposed representation, namely that both correspondingly modified scaling symmetries \bar{Q}_{NS} (5.44) and \bar{Q}_s (5.56) each must get broken

$$q_{\text{NS}} = 0, \quad q_s = 0, \quad (5.59)$$

when imposing the invariant constraint $\bar{U}_2^* = \bar{U}_2 = U_T$ in a consistent manner. Obviously, this constitutes a plausible result, because the full-field and the Reynolds-decomposed representation are ultimately equivalent to each other: Both must give the same mathematical and physical results with the same conclusions. Worthwhile to note in this regard is that, in contrast to the classical Navier-Stokes scaling symmetry \bar{T}_{NS} (5.29), which constitutes a consistent and well-defined symmetry, the new statistical scaling symmetry \bar{T}'_s (2.22), as first proposed in Khujadze & Oberlack (2004) and then later generalized in Oberlack & Rosteck (2010), is already inconsistent and thus unphysical by itself. For more details, we refer to Frewer *et al.* (2014, 2015).

For the sake of completeness, let us continue the inconsistent analysis as performed in Oberlack *et al.* (2015). This will lead us to another, independent mistake done therein. When re-writing the full-field invariant surface condition (5.35) into its Reynolds-decomposed form as proposed in Oberlack *et al.* (2015), namely by replacing the two full-field scaling symmetries \bar{T}'_s (2.22) and \bar{T}_{NS} (5.29) with their correspondingly modified Reynolds-decomposed scaling symmetries \bar{Q}_s (5.56) and \bar{Q}_{NS} (5.44), respectively, we obtain, for $q_s \neq 0$ and $q_{\text{NS}} \neq 0$, the following (inconsistent) invariant surface condition respecting the invariant constraint $\bar{U}_2^* = \bar{U}_2 = U_T$:

$$\begin{aligned} \frac{dx_1}{q_{\text{NS}}x_1 + k_{x_1}} &= \frac{dx_2}{q_{\text{NS}}x_2 + k_{x_2}} = \frac{d\bar{U}_i}{q_{\text{NS}}\phi_i + q_s\psi_i + \omega_i + \zeta_i + k_{\bar{U}_1}\delta_{1i}} = \frac{d\bar{P}}{q_{\text{NS}}\phi^p + q_s\psi^p + \omega^p + \zeta^p} \\ &= \frac{d(\partial_i\bar{P})}{q_{\text{NS}}\phi_i^p + q_s\psi_i^p + \omega_i^p + \zeta_i^p} = \frac{d\tau_{ij}}{q_{\text{NS}}\phi_{ij} + q_s\psi_{ij} + \omega_{ij} + \zeta_{ij}} \\ &= \frac{d\tau_{ijk}}{q_{\text{NS}}\phi_{ijk} + q_s\psi_{ijk} + \omega_{ijk} + \zeta_{ijk}} = \frac{d\overline{u_i\partial_j\bar{p}}}{q_{\text{NS}}\phi_{ij}^p + q_s\psi_{ij}^p + \omega_{ij}^p + \zeta_{ij}^p} \\ &= \frac{d\varepsilon_{ij}}{q_{\text{NS}}\phi_{ij}^v + q_s\psi_{ij}^v + \omega_{ij}^v + \zeta_{ij}^v}, \end{aligned} \quad (5.60)$$

which is identical to result [Eq. (354)][†] given in Oberlack *et al.* (2015), where the ϕ -terms result from the scaling symmetry \bar{Q}_{NS} (5.44) hierarchically given as

$$\left. \begin{aligned} \phi_i &= -\bar{U}_1\delta_{1i}, \quad \phi_{ij} = -2\tau_{ij} - 2\bar{U}_i\bar{U}_j - \phi_i\bar{U}_j - \phi_j\bar{U}_i, \\ \phi_{ijk} &= -3\tau_{ijk} - 3\left(\bar{U}_i\bar{U}_j\bar{U}_k + \bar{U}_i\tau_{jk} + \bar{U}_j\tau_{ik} + \bar{U}_k\tau_{ij}\right) - \phi_{ij}\bar{U}_k - \phi_{ik}\bar{U}_j - \phi_{jk}\bar{U}_i \\ &\quad - \phi_i\left(\tau_{jk} + \bar{U}_j\bar{U}_k\right) - \phi_j\left(\tau_{ik} + \bar{U}_i\bar{U}_k\right) - \phi_k\left(\tau_{ij} + \bar{U}_i\bar{U}_j\right), \\ \phi^p &= -2\bar{P}, \quad \phi_i^p = -3\partial_i\bar{P}, \quad \phi_{ij}^p = -4\overline{u_i\partial_j\bar{p}} - \bar{U}_i\frac{\partial\bar{P}}{\partial x_j} - \phi_i\frac{\partial\bar{P}}{\partial x_j}, \\ \phi_{ij}^v &= -4\varepsilon_{ij} - 4\nu\frac{\partial\bar{U}_i}{\partial x_2}\frac{\partial\bar{U}_j}{\partial x_2} - 2\nu\frac{\partial\phi_i}{\partial x_2}\frac{\partial\bar{U}_j}{\partial x_2} - 2\nu\frac{\partial\phi_j}{\partial x_2}\frac{\partial\bar{U}_i}{\partial x_2}, \end{aligned} \right\} \quad (5.61)$$

[†]Up to a non-essential linear combination in the translation symmetries and two misprints in the generator R_{12} , as mentioned in the points (i) and (iii) in the beginning of this subsection (p. 24), respectively. Further note that the correspondence of the parameters used in (5.60)-(5.64) to the ones defined in Oberlack *et al.* (2015) is: $k_{x_2} = k_{G,2}$, $q_{\text{NS}} = k_{\text{NS}}$, $q_s = k_s$, $c_1 = k_{\text{tr},1}$, $c_{ij} = k_{ij}$, and $k_{\bar{U}_1} = k_{z1}$.

the ψ -terms from the scaling symmetry \bar{Q}_s (5.56)

$$\left. \begin{aligned} \psi_i &= \bar{U}_1 \delta_{1i}, & \psi_{ij} &= \tau_{ij} + \bar{U}_i \bar{U}_j - \psi_i \bar{U}_j - \psi_j \bar{U}_i, \\ \psi_{ijk} &= \tau_{ijk} + \bar{U}_i \bar{U}_j \bar{U}_k + \bar{U}_i \tau_{jk} + \bar{U}_j \tau_{ik} + \bar{U}_k \tau_{ij} - \psi_{ij} \bar{U}_k - \psi_{ik} \bar{U}_j - \psi_{jk} \bar{U}_i \\ &\quad - \psi_i (\tau_{jk} + \bar{U}_j \bar{U}_k) - \psi_j (\tau_{ik} + \bar{U}_i \bar{U}_k) - \psi_k (\tau_{ij} + \bar{U}_i \bar{U}_j), \\ \psi^p &= \bar{P}, & \psi_i^p &= \partial_i \bar{P}, & \psi_{ij}^p &= \overline{u_i \partial_j \bar{P}} - \psi_i \frac{\partial \bar{P}}{\partial x_j}, \\ \psi_{ij}^\nu &= \varepsilon_{ij} + 2\nu \frac{\partial \bar{U}_i}{\partial x_2} \frac{\partial \bar{U}_j}{\partial x_2} - 2\nu \frac{\partial \psi_i}{\partial x_2} \frac{\partial \bar{U}_j}{\partial x_2} - 2\nu \frac{\partial \psi_j}{\partial x_2} \frac{\partial \bar{U}_i}{\partial x_2}, \end{aligned} \right\} (5.62)$$

the ω -terms from the linear superposition symmetry \bar{T}'_+ (5.30) with the specification (5.34)

$$\left. \begin{aligned} \omega_i &= 0, \\ \omega_{ij} &= 2k_{z11} x_2 \delta_{1i} \delta_{1j} + 2k_{z22} x_2 \delta_{2i} \delta_{2j} + 2k_{z33} x_2 \delta_{3i} \delta_{3j} + k_{z12} x_2 (\delta_{1i} \delta_{2j} + \delta_{1j} \delta_{2i}), \\ \omega_{ijk} &= 0, & \omega^p &= -k_{z12} x_1 - 2k_{z22} x_2, & \omega_i^p &= -k_{z12} \delta_{1i} - 2k_{z22} \delta_{2i}, \\ \omega_{ij}^p &= k_{z12} \bar{U}_i \delta_{1j} + 2k_{z22} \bar{U}_i \delta_{2j}, & \omega_{ij}^\nu &= 0, \end{aligned} \right\} (5.63)$$

and finally the ζ -terms resulting from the translation symmetry \bar{T}'_c (2.26)

$$\left. \begin{aligned} \zeta_i &= c_1 \delta_{1i}, & \zeta_{ij} &= -\zeta_i \bar{U}_j - \zeta_j \bar{U}_i + c_{ij}, \\ \zeta_{ijk} &= -\zeta_{ij} \bar{U}_k - \zeta_{ik} \bar{U}_j - \zeta_{jk} \bar{U}_i \\ &\quad - \zeta_i (\tau_{jk} + \bar{U}_j \bar{U}_k) - \zeta_j (\tau_{ik} + \bar{U}_i \bar{U}_k) - \zeta_k (\tau_{ij} + \bar{U}_i \bar{U}_j) + c_{ijk}, \\ \zeta^p &= d, & \zeta_i^p &= 0, & \zeta_{ij}^p &= -\zeta_i \frac{\partial \bar{P}}{\partial x_j}, & \zeta_{ij}^\nu &= 0. \end{aligned} \right\} (5.64)$$

Note that (5.60) coherently extends the condition in Oberlack *et al.* (2015) up to third order in the velocity correlations, including the moments for pressure and dissipation.

Anyhow, although the required constraint of a mean constant and invariant wall-normal velocity $\bar{U}_2^* = \bar{U}_2 = U_T$ has been (inconsistently) implemented into the invariant surface condition (5.60) without breaking a scaling symmetry, i.e. for $q_{NS} \neq 0$ and $q_s \neq 0$, this has not been done for the second required system constraint, namely that of a mean constant and invariant streamwise pressure gradient $\partial \bar{P}^* / \partial x_1^* = \partial \bar{P} / \partial x_1 = -K$. Because, when this constraint $d(\partial_1 \bar{P}) = 0$ is applied to (5.60), it will unavoidably result into the two symmetry breaking constraints

$$q_{NS} \phi_1^p + q_s \psi_1^p = 0, \quad \text{and} \quad \omega_1^p = 0, \quad (5.65)$$

which equivalently turn into the restrictions

$$q_s = 3q_{NS}, \quad \text{and} \quad k_{z12} = 0, \quad (5.66)$$

an important result not obtained in Oberlack *et al.* (2015). The reason of why this result (5.66) was not obtained, is that in Oberlack *et al.* (2015) a second, independent mistake was made: Instead of correctly determining the invariant mean pressure gradient $\partial_i \bar{P}$ as a function of x_2 in the wall-normal and as a constant in the streamwise direction via its invariant surface condition (5.60), it was incorrectly determined as a functional residual of the two momentum equations (5.45), namely as

$$\frac{\partial \bar{P}}{\partial x_1} = -U_T \frac{\partial \bar{U}_1^{\text{inv}}}{\partial x_2} - \frac{\partial \tau_{12}^{\text{inv}}}{\partial x_2} + \nu \frac{\partial^2 \bar{U}_1^{\text{inv}}}{\partial x_2^2}, \quad \text{and} \quad \frac{\partial \bar{P}}{\partial x_2} = -\frac{\partial \tau_{22}^{\text{inv}}}{\partial x_2}, \quad (5.67)$$

where the parameters for the already determined invariant solutions of (5.60), \bar{U}_1^{inv} , τ_{12}^{inv} and τ_{22}^{inv} , were then arranged such that $\partial\bar{P}/\partial x_1$ is a constant and $\partial\bar{P}/\partial x_2$ only a function of x_2 . The reason why the latter procedure is incorrect, is that it is decisively incomplete: The relations in (5.67) only give constraint conditions among the parameters of the invariant solutions \bar{U}_1^{inv} , τ_{12}^{inv} and τ_{22}^{inv} , under the *assumption* of a constant pressure gradient $\partial\bar{P}/\partial x_1 = -K$ in the streamwise and a sole x_2 -dependence $\partial\bar{P}/\partial x_2 = \mathcal{G}(x_2)$ in the wall-normal direction. But, these relations do *not* warrant that the determined pressure $\bar{P} = \bar{P}(x_1, x_2)$ from (5.67), with gradient $\partial_i\bar{P} = -K\delta_{1i} + \mathcal{G}(x_2)\delta_{2i}$, constitutes an invariant function by itself, being compatible to the invariant pressure solution $\bar{P}^{\text{inv}} = \bar{P}^{\text{inv}}(x_1, x_2)$ obtained from the invariant surface condition (5.60) with gradient $\partial_i\bar{P}^{\text{inv}} = -K\delta_{1i} + \mathcal{G}^{\text{inv}}(x_2)\delta_{2i}$. In other words, the pressure solution \bar{P} obtained from (5.67) is in general not an invariant function under all symmetries considered, and thus in general not compatible to the invariant pressure solution \bar{P}^{inv} obtained from (5.60). Generally speaking, the reason for this is that the residuals (5.67) do not constitute invariant relations, since the coordinates x_1 and x_2 themselves do not constitute invariant quantities. Hence, instead of the incomplete and thus in general incorrect relations (5.67) as considered in Oberlack *et al.* (2015), the following complete and correct relations have to be inquired

$$\frac{\partial\bar{P}^{\text{inv}}}{\partial x_1} = -U_T \frac{\partial\bar{U}_1^{\text{inv}}}{\partial x_2} - \frac{\partial\tau_{12}^{\text{inv}}}{\partial x_2} + \nu \frac{\partial^2\bar{U}_1^{\text{inv}}}{\partial x_2^2}, \quad \frac{\partial\bar{P}^{\text{inv}}}{\partial x_2} = -\frac{\partial\tau_{22}^{\text{inv}}}{\partial x_2}, \quad (5.68)$$

which now not only give the correct and consistent constraint conditions among the parameters of *all* invariant solutions involved, but which will also give, in general, *more* constraint conditions than the (inconsistent) relations (5.67) may give, simply because the invariant-based system constraint for (5.68), $\partial_i\bar{P}^{\text{inv}} = -K\delta_{1i} + \mathcal{G}^{\text{inv}}(x_2)\delta_{2i}$, is in general more restrictive than the constraint $\partial_i\bar{P} = -K\delta_{1i} + \mathcal{G}(x_2)\delta_{2i}$ for (5.67). For example, for the case presently studied, (5.67) will only give one non-zero-constraint, [Eq. (361)] *or* [Eq. (365)][†] in Oberlack *et al.* (2015), while (5.68) will not only give more non-zero-constraints, but, additionally, also two pivotal constraints, namely exactly those two already obtained before in (5.66).

The methodological mistake done in Oberlack *et al.* (2015), namely to consider (5.67) and not (5.68), is critical to their conclusions: (i) Since the correct relation (5.68) will give the constraint $q_s = 3q_{\text{NS}}$ (5.66), no logarithmic scaling law for the mean velocity profile \bar{U}_1 can be derived as incorrectly claimed in Oberlack *et al.* (2015), because the ansatz $q_s = q_{\text{NS}}$ would then only lead to $q_s = q_{\text{NS}} = 0$. Hence, only an algebraic invariant solution for \bar{U}_1 can be generated. (ii) In their “algebraic solution” [Eq. (382)] for $k_s \neq 3k_{\text{NS}}$, the second constraint $k_{z12} = 0$ from (5.68) will give the analytical result $D_{12} = 0$, being different to their DNS-matched value $D_{12} \sim 1$ [Table 10]. Hence, since D_{12} represents the mean streamwise pressure gradient, the constraint $k_{z12} = 0$ thus can only go along with the constraint $k_s = 3k_{\text{NS}}$, in order to generate a non-zero streamwise pressure gradient.

In the following we repeat the (inconsistent) analysis of Oberlack *et al.* (2015), in generating several invariant solutions from (5.60) and matching them to the DNS data of Avsarkisov *et al.* (2014), however, only for the correctly posed constraints (5.66). For $q_{\text{NS}} \neq 0$ and $q_s \neq 0$, we yield from (5.60) with (5.66) only a quadratic power-law for the mean invariant velocity profile as

$$\bar{U}_1(x_2) = B_1 + C_1 \left(\frac{x_2}{h} + A \right)^2, \quad (5.69)$$

where we use the parameter notation of Oberlack *et al.* (2015): The parameters A and B_1 are

[†]To note is that the result for the invariant solution \tilde{R}_{12} [Eq. (363)] in Oberlack *et al.* (2015) misses the summand $U_T k_{z12} k_{G,2} / (k_{\text{NS}}(k_{G,2} + k_{\text{NS}}x_2))$, but which apparently was absorbed into the term $C_{I,12} / (k_{G,2} + k_{\text{NS}}x_2)$ of the arbitrary integration constant $C_{I,12}$, while the result for the invariant solution \tilde{R}_{22} carries the wrong sign in the U_T^2 -term.

given by [Eq. (379)],[†] as $A = k_{x_2}/(hq_{\text{NS}})$ and $B_1 = -(k_{\bar{U}_1} + c_1)/(2q_{\text{NS}})$, while C_1 is an arbitrary integration constant. Note the striking difference that for the presently considered viscous case ($\nu \neq 0$), the consistent and correct scaling law for the mean velocity profile (5.69) carries one (matching) parameter less than the correspondingly derived (inconsistent) scaling law [Eq. (380)] in Oberlack *et al.* (2015). A consistent analysis shows that $\gamma = 2$, in clear contrast to the non-positive and non-constantly matched values for γ in Oberlack *et al.* (2015) [Table 10], where the algebraic scaling coefficient γ is declared to be a non-positive and dependent function on the transpiration rate and the Reynolds number: $\gamma = \gamma(U_T^+, Re_\tau) < 0$.

With the result (5.69), all remaining invariant solutions can be determined from (5.60) with (5.66) accordingly. For example, the invariant Reynolds stresses are given as

$$\left. \begin{aligned} \tau_{ij}(x_2) &= \beta_{ij} \left(\frac{x_2}{h} + A \right) - \bar{U}_i \bar{U}_j + \sigma_{ij} \left(\frac{x_2}{h} + A \right) \ln \left(\frac{x_2}{h} + A \right) + \rho_i \bar{U}_j + \rho_j \bar{U}_i + \alpha_{ij}, \\ \tau_{13}(x_2) &= 0, \quad \tau_{23}(x_2) = 0, \end{aligned} \right\} \quad (5.70)$$

where all β 's are arbitrary integration constants,[‡] while the remaining parameters are determined through the group constants as

$$\left. \begin{aligned} \sigma_{ij} &= \frac{2h(k_{z11}\delta_{1i}\delta_{1j} + k_{z22}\delta_{2i}\delta_{2j} + k_{z33}\delta_{3i}\delta_{3j})}{q_{\text{NS}}}, \quad \rho_i = \frac{k_{\bar{U}_1}}{q_{\text{NS}}}\delta_{1i}, \\ \alpha_{ij} &= \sigma_{ij}A - \frac{k_{\bar{U}_1}(4B_1\delta_{1i}\delta_{1j} + 2U_T(\delta_{1i}\delta_{2j} + \delta_{1j}\delta_{2i}))}{q_{\text{NS}}} - \frac{c_{ij}}{q_{\text{NS}}}. \end{aligned} \right\} \quad (5.71)$$

An interesting measure to verify the predictability of the invariant functions from (5.60) is the dissipation, which is given as

$$\varepsilon_{ij}(x_2) = \mu_{ij} \left(\frac{x_2}{h} + A \right)^{-1} - 2\nu \left(\frac{\partial \bar{U}_1}{\partial x_2} \right)^2 \delta_{1i}\delta_{1j}, \quad (5.72)$$

where the μ 's are again arbitrary integration constants. For the statistical DNS data available from Avsarkisov *et al.* (2014), we can only compare to the scalar dissipation defined as

$$\begin{aligned} \varepsilon &:= \frac{1}{2} \sum_{i=1}^3 \varepsilon_{ii} = \frac{1}{2} \sum_{i=1}^3 \left[\mu_{ij} \left(\frac{x_2}{h} + A \right)^{-1} - 2\nu \left(\frac{\partial \bar{U}_1}{\partial x_2} \right)^2 \delta_{1i}\delta_{1j} \right] \\ &\equiv \mu \left(\frac{x_2}{h} + A \right)^{-1} - \nu \left(\frac{\partial \bar{U}_1}{\partial x_2} \right)^2, \end{aligned} \quad (5.73)$$

which, since it was only calculated in the u_τ -normalized form, has to be transformed accordingly

$$\begin{aligned} \varepsilon^+ &= \frac{1}{2} \sum_{i=1}^3 \varepsilon_{ii}^+ = \frac{1}{2} \sum_{i=1}^3 2 \frac{\overline{\partial u_i^+}}{\partial x_k^+} \frac{\partial u_i^+}{\partial x_k^+} = \frac{\nu}{u_\tau^4} \cdot \frac{1}{2} \sum_{i=1}^3 2\nu \frac{\overline{\partial u_i}}{\partial x_k} \frac{\partial u_i}{\partial x_k} = \frac{\nu}{u_\tau^4} \cdot \frac{1}{2} \sum_{i=1}^3 \varepsilon_{ii} = \frac{\nu}{u_\tau^4} \cdot \varepsilon \\ &= \mu^+ \left(\frac{x_2}{h} + A \right)^{-1} - \frac{4C_1^{+2}}{Re_\tau^2} \left(\frac{x_2}{h} + A \right)^2. \end{aligned} \quad (5.74)$$

[†][Eq. (379)] in Oberlack *et al.* (2015) contains two misprints: The parameter A is missing a factor $1/h$ to be dimensionally correct, and in C_1 the non-constant $k_{\text{NS}} x_2^{k_s/k_{\text{NS}}-1}$ has to be replaced by $k_{\text{NS}}^{k_s/k_{\text{NS}}-1}$. Moreover, in [Eq. (380)], and as well as in [Eq. (384)], all field variables were misleadingly denoted in dimensionless “+”-units, although the functional expressions themselves are not normalized on u_τ . Finally note that B_1 in [Eq. (379)] differs by one translation group parameter to ours defined in (5.69). As already mentioned in point (i) in the beginning of this subsection (p. 24), the reason is that in Oberlack *et al.* (2015) a different but equivalent linear combination of the two independent translation symmetries is considered.

[‡]Full arbitrariness in all parameters, however, is not given, since certain consistency relations have to be satisfied from the underlying statistical equations (5.45)-(5.46). For example, the parameter β_{12} is not arbitrary, but determined as $\beta_{12} = u_\tau^2 + 2C_1 u_\tau / Re_\tau$.

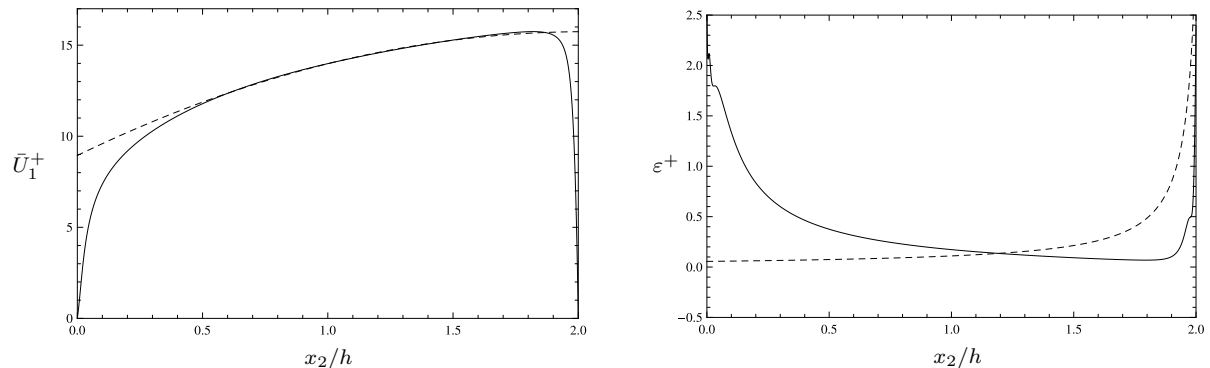


Figure 8: Matching of the two theoretically predicted scaling laws for the (normalized) mean velocity field \bar{U}_1^+ (5.69) and the scalar dissipation ϵ^+ (5.74) to the DNS data of Avsarkisov *et al.* (2014) for $Re_\tau = 480$ and $v_0^+ = 0.10$. The DNS data is displayed by solid lines, the corresponding scaling laws by dashed lines. The matching region $0.5 \leq x_2/h \leq 1.6$ has been taken over from the result determined in Oberlack *et al.* (2015) as listed in [Table 9]. The resulting best-fitted parameters are given as: $A = -2.035$, $B_1^+ = 15.74$, $C_1^+ = -1.643$ and $\mu^+ = -0.114$. While the fitting for \bar{U}_1^+ is more or less satisfactory, the fitting of ϵ^+ fails.

To note is that the above scaling law only has one free matching parameter μ^+ , since A and C_1^+ are determined by the scaling law (5.69) of the normalized mean velocity field \bar{U}_1^+ . Hence, the scalar dissipation ϵ^+ will thus be the ultimate litmus test in how far the Lie-group-based scaling theory, as currently proposed in Oberlack *et al.* (2015), is able to consistently predict the scaling behavior of Navier-Stokes turbulence. As to be expected from the investigation done in this section, the proposed theory fails: As shown in Figure 8, the scaling law (5.74) for the scalar dissipation ϵ^+ fails to even roughly predict the tendency of the DNS data, although for the lowest order moment, the mean velocity field \bar{U}_1^+ , the scaling law (5.69) was matched more or less satisfactorily.[†]

The reason for this failure is clear: The considered invariant surface condition (5.60), as proposed in Oberlack *et al.* (2015), involves two unphysical scaling symmetries, namely \bar{Q}_{NS} (5.44) and \bar{Q}_s (5.56), which both are inconsistent to the underlying deterministic theory in violating the classical principle of cause and effect. As a consequence, the theoretically predicted scaling behavior of the lowest order moment \bar{U}_1^+ is incompatible to the scaling behavior of the higher-order moment ϵ^+ , as clearly seen in Figure 8, an incompatibility which also runs through all other higher-order moments.

6. Summary and conclusion

The main motivation of this investigation was to reveal in how far the study of Avsarkisov *et al.* (2014) is reproducible. With the data made available on their institutional website [fdy], we failed to reproduce Fig. 9 (a) & (c) in Avsarkisov *et al.* (2014). The critical conclusions made from these figures can not be confirmed from our analysis: Neither do the mean velocity profiles (in deficit form) universally collapse onto a single curve for different transpiration rates at a constant Reynolds number (Fig. 9 (a)), nor does the universally proposed logarithmic scaling law in the center of the channel match the DNS data for the presented parameter values (Fig. 9 (c)).

No universal scaling behavior in the center of the channel can be detected as claimed in Avsarkisov *et al.* (2014), not even when considering the case of a constant transpiration rate at different Reynolds numbers, which led to the incorrect assumption to only conduct a Reynolds-number independent symmetry analysis. Because, as we have demonstrated several times, such

[†]That the scaling law (5.69) for the mean velocity field can be matched more or less satisfactorily, is not surprising, since this law involves three independent matching parameters, while the scaling law (5.74) for the scalar dissipation only involves one free parameter.

an assumption, of an inviscid ($\nu = 0$) and thus Reynolds-number independent symmetry analysis, is not justified to consistently predict the scaling behavior of a channel flow with uniform wall-normal transpiration for the flow conditions considered. In particular, we revealed that the associated Re_τ -independent scaling group parameter for the mean velocity field was inconsistently matched in Avsarkisov *et al.* (2014) to a Re_τ -dependent quantity, being proportional to u_τ , which, as clearly shown in Figure 6, or Table 3, inevitably leads to a strong Re_τ -dependence in all invariant scaling laws when extending the scaling theory of Avsarkisov *et al.* (2014) coherently to higher orders beyond the mean velocity moment. Hence, a consistent symmetry analysis to all orders can only be achieved when also including the viscous terms. This has been attempted in their subsequent study Oberlack *et al.* (2015).

But, both the inviscid ($\nu = 0$) as well as the viscous ($\nu \neq 0$) symmetry analysis, performed in Avsarkisov *et al.* (2014) and Oberlack *et al.* (2015), respectively, is inconsistent *per se*.[†] As explained and discussed in the previous section, this inconsistency is due to that both their investigations involve several unphysical symmetries that are inconsistent with the underlying deterministic description of turbulence, in that they violate the classical principle of cause and effect: The former inviscid analysis in Avsarkisov *et al.* (2014) (when extended to higher-order moments) involves two unphysical symmetries, namely \bar{T}'_s (2.17) and \bar{T}'_c (2.26), while the latter symmetry analysis in Oberlack *et al.* (2015) involves three unphysical symmetries, \bar{Q}_{NS} (5.44),[‡] \bar{Q}_s (5.56) and again \bar{T}'_c (2.26). The consequence: Any derived set of invariant solutions beyond the lowest-order moment cannot be consistently matched to the DNS data anymore, as clearly shown in Figure 4 & 8 for the inviscid and viscous symmetry analysis, respectively. In particular the matching of the scalar dissipation, being a critical indicator to judge the prediction quality of any theoretically proposed scaling laws, failed exceedingly. To gain the mathematical insight into the reason for this failure, we refer to our foregoing publications Frewer *et al.* (2014); Frewer (2015a,b); Frewer *et al.* (2015) and Frewer *et al.* (2016).

A. Friction velocity from both walls as a measure of the pressure gradient

In a canonical turbulent channel flow of height $2h$ without wall-normal transpiration, driven by a mean constant streamwise pressure gradient $-\partial\bar{P}/\partial x_1 = K > 0$, between $x_2 = 0$ (lower plate) and $x_2 = 2h$ (upper plate), the squared friction velocity (normalized on the density ρ)

$$u_\tau^2 = \tau|_{x_2=0} = -\tau|_{x_2=2h} > 0, \quad (\text{A.1})$$

where $\tau = \tau(x_2)$ being the total mean shear stress

$$\tau = -\overline{u_1 u_2} + \nu \frac{d\bar{U}_1}{dx_2}, \quad (\text{A.2})$$

is simply determined by the pressure gradient and the half-width of the channel only (see. e.g. (Tennekes & Lumley, 1972))

$$u_\tau^2 = K \cdot h, \quad (\text{A.3})$$

due to the fact that at the center of the channel ($x_2 = h$) the total shear stress is zero, i.e., $\tau|_{x_2=h} = 0$, for reasons of symmetry. In particular, this result (A.3) is obtained by integrating the mean streamwise momentum equation from the lower plate upwards

$$0 = \int_0^{x_2} \left(K + \frac{d\tau}{dx'_2} \right) dx'_2 = Kx_2 + \tau - \tau|_{x_2=0} = Kx_2 + \tau - u_\tau^2, \quad (\text{A.4})$$

[†]Apart from the additional fact that the symmetry analysis in Oberlack *et al.* (2015) is also technically flawed, in that a wrong and not enough constraint relations from the statistical momentum equations are determined which incorrectly allow for a logarithmic as well as an algebraic invariant solution in the mean velocity field. Instead, a correct analysis reveals that only an algebraic invariant solution of quadratic type can be obtained. And when excluding even the unphysical symmetries, then only a featureless linear profile is obtained.

[‡]Recall again that, although the artificially constructed and unphysical statistical symmetry \bar{Q}_{NS} (5.44) is motivated from the well-known single physical scaling symmetry of the Navier-Stokes equations \bar{T}_{NS} (5.29), there is no connection between them.

which then reduces to (A.3) when evaluated at $x_2 = h$. However, when considering a turbulent channel flow with uniform wall-normal transpiration v_0 , the total shear stress (including the shear stress from the transpiration)

$$\mathcal{T} = \tau - v_0 \bar{U}_1, \quad (\text{A.5})$$

is obviously not zero anymore at the center of the channel, i.e., $\mathcal{T}|_{x_2=h} \neq 0$, but rather at some different, yet unknown height position $x_2 = x_2^*$ somewhere inside the channel, i.e., $\mathcal{T}|_{x_2=x_2^*} = 0$. Although not knowing this position $0 \leq x_2^* \leq 2h$, one nevertheless can derive the same relation (A.3) in an averaged sense by considering the different shear stresses on both walls. Because, by first integrating the mean streamwise momentum equation once from the lower plate up to the unknown position

$$\begin{aligned} 0 &= \int_0^{x_2^*} \left(K + \frac{d\mathcal{T}}{dx_2} \right) dx_2 = Kx_2^* + \mathcal{T}|_{x_2=x_2^*} - \mathcal{T}|_{x_2=0} = Kx_2^* - \mathcal{T}|_{x_2=0} \\ &= Kx_2^* - \tau|_{x_2=0}, \end{aligned} \quad (\text{A.6})$$

and once from the unknown position up to the upper plate

$$\begin{aligned} 0 &= \int_{x_2^*}^{2h} \left(K + \frac{d\mathcal{T}}{dx_2} \right) dx_2 = 2Kh - Kx_2^* + \mathcal{T}|_{x_2=2h} - \mathcal{T}|_{x_2=x_2^*} = 2Kh - Kx_2^* + \mathcal{T}|_{x_2=2h} \\ &= 2Kh - Kx_2^* + \tau|_{x_2=2h}, \end{aligned} \quad (\text{A.7})$$

and then by adding both relations, we obtain the x_2^* -independent result

$$0 = 2Kh + \tau|_{x_2=2h} - \tau|_{x_2=0}, \quad (\text{A.8})$$

which, according to the initial definition (A.1), finally turns into

$$Kh = \frac{\tau|_{x_2=0} - \tau|_{x_2=2h}}{2} = u_{\tau}^2, \quad (\text{A.9})$$

where we then have, according to (A.2),

$$u_{\tau b}^2 := \tau_{wb} := \tau|_{x_2=0} = \nu \frac{d\bar{U}_1}{dx_2} \Big|_{x_2=0}, \quad u_{\tau s}^2 := \tau_{ws} := -\tau|_{x_2=2h} = -\nu \frac{d\bar{U}_1}{dx_2} \Big|_{x_2=2h}, \quad (\text{A.10})$$

the wall shear stresses at the blowing (b) and the suction (s) wall, respectively, and thus overall coinciding with the result [Eq. (2.1)] given in Avsarkisov *et al.* (2014).

B. Laminar channel flow with uniform wall transpiration[†]

The governing equations are the incompressible Navier-Stokes equations

$$\left. \begin{aligned} \frac{\partial U_k}{\partial x_k} &= 0, \\ \frac{\partial U_i}{\partial t} + U_j \frac{\partial U_i}{\partial x_j} &= -\frac{\partial P}{\partial x_i} + \nu \Delta U_i, \end{aligned} \right\} \quad (\text{B.1})$$

which considerably reduces in dimension when considering a stationary laminar channel flow of width $2h$ driven by a constant streamwise pressure gradient $K > 0$. When additionally considering permeable walls in which a uniform wall-normal flow $v_0 > 0$ is injected at the lower

[†]Alternative derivations for laminar solutions under these flow conditions can also be found, e.g., in Chang (2009) or in Avsarkisov (2013).

wall (the blowing side $x_2 = 0$) to be then also fully uniformly sucked out at the upper wall (the suction side $x_2 = 2h$), the overall flow conditions will read:

$$U_1 = U_1(x_2), \quad U_2 = v_0, \quad U_3 = 0, \quad -\frac{\partial P}{\partial x_1} = K, \quad U_1(x_2 = 0) = U_1(x_2 = 2h) = 0, \quad (\text{B.2})$$

for which the Navier-Stokes equations (B.1) will reduce to the single equation

$$v_0 \frac{dU_1(x_2)}{dx_2} = K + \nu \frac{d^2U_1(x_2)}{dx_2^2}, \quad \text{with } U_1(0) = U_1(2h) = 0. \quad (\text{B.3})$$

Two things should be pointed out: (i) If the dependent variable U_1 is not normalized, then equation (B.3) consists of three parameters which can be varied independently, the transpiration rate v_0 , the driving force K and the viscosity ν . This threefold independent variation turns out to be necessary when normalizing according to procedure outlined in Avsarkisov *et al.* (2014). (ii) The DNS in Avsarkisov *et al.* (2014) was performed under the additional constraint of a constant mass flux.[†] This constraint was applied globally (universally) for all different initially chosen transpiration rates and Reynolds numbers. Now, since every DNS can also simulate laminar solutions as a special case, we will construct these in accord with the simulation performed in Avsarkisov *et al.* (2014), i.e., we will construct the set of all laminar solutions under the additional universal constraint of a constant mass flux $Q = Q^*$, where

$$Q = \rho \cdot \frac{1}{2h} \int_0^{2h} U_1(x_2) dx_2 =: \rho \cdot U_B. \quad (\text{B.4})$$

Instead of Q we can also equivalently consider the bulk velocity U_B (since the density ρ is treated here as constant which can be absorbed into Q , similar to the pressure P in (B.1) which is also normalized relative to ρ). Note that only the mass flux in the streamwise direction needs to be considered, since in the wall-normal direction the mass flux is already constant by construction. Hence, next to equation (B.3) we thus have to also consider the equation of a universally fixed bulk velocity $U_B = U_B^*$

$$U_B^* = \frac{1}{2h} \int_0^{2h} U_1(x_2) dx_2, \quad (\text{B.5})$$

that is, equation (B.3) needs to be solved such that the constraint is always universally satisfied for all different initially chosen parameters v_0 , K and ν . The particular value U_B^* can be chosen arbitrarily from the outset, but once chosen, it is universally fixed and cannot change anymore during solution construction.

Before we explicitly solve equation (B.3) under the constraint (B.5), it is advantageous to normalize the expressions appropriately. Two interrelated but different normalization choices exist: The first one is based on U_B^* along with h (for the independent spatial coordinate). The system (B.3) and (B.5) then turns into

$$\frac{v_0}{U_B^* \cdot h} \frac{dU_1(x_2/h \cdot h)}{d(x_2/h)} = \frac{K}{U_B^*} + \frac{\nu}{U_B^* \cdot h^2} \frac{d^2U_1(x_2/h \cdot h)}{d(x_2/h)^2}, \quad \text{with } U_1(0/h \cdot h) = U_1(2h/h \cdot h) = 0,$$

$$U_B^* = \frac{1}{2h} h \int_{0/h}^{2h/h} U_1(x_2/h \cdot h) d(x_2/h),$$

which, in terms of the dimensionless spatial coordinate $x'_2 = x_2/h$, can be equivalently written as

$$\left. \begin{aligned} v_0^B \frac{d\hat{U}_1(x'_2)}{dx'_2} &= w_K^B + \frac{1}{Re_B} \frac{d^2\hat{U}_1(x'_2)}{dx'^2}, \quad \text{with } \hat{U}_1(0) = \hat{U}_1(2) = 0, \\ U_B^* &= \frac{1}{2} \int_0^2 \hat{U}_1(x'_2) dx'_2, \end{aligned} \right\} \quad (\text{B.6})$$

[†]To maintain during simulation a constant mass flux in each time step, the pressure gradient has to adapt accordingly. However, since we are only interested in the statistically stationary state, the pressure gradient will still average out to a constant in the streamwise direction, but in each case to different values for different transpiration rates and Reynolds numbers.

where $v_0^B = v_0/U_B^*$, $w_K^B = Kh/U_B^*$ and $Re_B = U_B^*h/\nu$ are the (relative to the bulk velocity) normalized transpiration rate, the pressurized forcing rate and the bulk Reynolds number, respectively. Note that system (B.6) is yet not fully normalized, since $\hat{U}_1(x'_2)$ still carries the dimension of velocity. Obviously, this quantity can be normalized by the remaining constant velocity scale w_K^B , but in this final step we have to bear in mind that the parameter w_K^B is explicitly needed to satisfy the constraint equation $U_B = U_B^*$. Hence, only a partial normalization may be performed in which w_K^B is not completely absorbed by both equations. This will turn (B.6) into the equivalent system

$$\left. \begin{aligned} v_0^B \frac{d\hat{U}_1^w(x'_2)}{dx'_2} &= 1 + \frac{1}{Re_B} \frac{d^2\hat{U}_1^w(x'_2)}{dx'^2}, \quad \text{with } \hat{U}_1^w(0) = \hat{U}_1^w(2) = 0, \\ w_K^B &= \frac{U_B^*}{\frac{1}{2} \int_0^2 \hat{U}_1^w(x'_2) dx'_2}, \end{aligned} \right\} \quad (\text{B.7})$$

where $\hat{U}_1^w = \hat{U}_1/w_K^B$ is the normalized (dimensionless) velocity field relative to the velocity scale $w_K^B \sim K$ being a measure of the pressure gradient K . As already pointed out in the beginning of this section, three independent parameters need to be initialized in order to solve (B.7): v_0^B , Re_B and U_B^* , representing ultimately the transpiration rate v_0 , the viscosity ν and indirectly, via $U_B^* \sim w_K^B$, the pressure gradient K , respectively. Note that the fully normalized system (B.7) is uncoupled: The first equation gives \hat{U}_1^w , which then immediately yields the consistent value for the unknown scale w_K^B by just evaluating the right-hand side of the second equation.

The second normalization is based on u_τ , as defined through [Eq. (2.1)] in Avsarkisov *et al.* (2014), and again along with h for the spatial coordinate. For this choice, system (B.3) and (B.5) turns into

$$\begin{aligned} \frac{v_0}{u_\tau \cdot h} \frac{dU_1(x_2/h \cdot h)}{d(x_2/h)} &= \frac{K}{u_\tau} + \frac{\nu}{u_\tau \cdot h^2} \frac{d^2U_1(x_2/h \cdot h)}{d(x_2/h)^2}, \quad \text{with } U_1(0/h \cdot h) = U_1(2h/h \cdot h) = 0, \\ U_B^* &= \frac{1}{2h} h \int_{0/h}^{2h/h} U_1(x_2/h \cdot h) d(x_2/h), \end{aligned}$$

which then, again in terms of the dimensionless spatial coordinate $x'_2 = x_2/h$, can be equivalently written as

$$\left. \begin{aligned} v_0^+ \frac{d\hat{U}_1(x'_2)}{dx'_2} &= u_\tau + \frac{1}{Re_\tau} \frac{d^2\hat{U}_1(x'_2)}{dx'^2}, \quad \text{with } \hat{U}_1(0) = \hat{U}_1(2) = 0, \\ U_B^* &= \frac{1}{2} \int_0^2 \hat{U}_1(x'_2) dx'_2, \end{aligned} \right\} \quad (\text{B.8})$$

where $u_\tau = \sqrt{Kh}$, $v_0^+ = v_0/u_\tau$ and $Re_\tau = u_\tau h/\nu$ are the friction velocity (measured relative to the constant streamwise pressure gradient $K > 0$), the transpiration rate based on this scale u_τ and friction Reynolds number, respectively. Note again that at this stage system (B.8) is yet not fully normalized, since $\hat{U}_1(x'_2)$ still carries the dimension of velocity. Similarly as discussed before for the first normalization choice, $\hat{U}_1(x'_2)$ can be obviously normalized by the constant velocity scale u_τ , but in this step we have to bear in mind again that the parameter u_τ is explicitly needed to satisfy the constraint equation $U_B = U_B^*$. Hence, again, only a partial normalization may be performed in which u_τ may not be completely absorbed by both equations. This will turn (B.8) into the equivalent system

$$\left. \begin{aligned} v_0^+ \frac{d\hat{U}_1^+(x'_2)}{dx'_2} &= 1 + \frac{1}{Re_\tau} \frac{d^2\hat{U}_1^+(x'_2)}{dx'^2}, \quad \text{with } \hat{U}_1^+(0) = \hat{U}_1^+(2) = 0, \\ u_\tau &= \frac{U_B^*}{\frac{1}{2} \int_0^2 \hat{U}_1^+(x'_2) dx'_2}, \end{aligned} \right\} \quad (\text{B.9})$$

		Turbulent flow	Laminar flow
Re_τ	v_0^+	v_0/U_B^*	v_0^L/U_B^*
250	0.05	0.0030	0.0027
250	0.10	0.0069	0.0104
250	0.16	0.0164	0.0263
250	0.26	0.0500	0.0687
250	∞		∞
480	0.05	0.0030	0.0026
480	0.10	0.0075	0.0102
480	0.16	0.0164	0.0259
480	0.26	0.0490	0.0681
480	∞		∞
850	0.05	0.0026	0.0026
850	0.16	0.0160	0.0258
∞	$v_0^+ \neq 0$		v_0^{+2}
∞	∞		∞

Table 4: Calculated values for v_0/U_B^* for initially given Re_τ and v_0^+ . The values for the turbulent case were taken from Table 1 [p. 106] in Avsarkisov *et al.* (2014), while the values for the corresponding laminar case were calculated according to the analytical relation (B.13), where we denoted the dimensionalized transpiration rate as v_0^L to distinguish it from the turbulent flow condition.

where $\hat{U}_1^+ = \hat{U}_1/u_\tau$ is the normalized (dimensionless) velocity field relative to the velocity scale $u_\tau \sim \sqrt{K}$ being again a measure of the pressure gradient K . As was also already discussed before, three independent parameters need to be given again in order to solve the (uncoupled) system (B.9): Two, namely v_0^+ and Re_τ , in the beginning to solve the first equation and then one, namely U_B^* , in the end to evaluate the second expression in order to obtain the consistent value for the unknown scale u_τ .

The two different normalization choices just discussed above are, of course, interrelated. That is, system (B.7) can be bijectively mapped to system (B.9) and vice versa. The relations are: $v_0^B/v_0^+ = u_\tau/U_B^*$ and $Re_B/Re_\tau = \hat{U}_1^w/\hat{U}_1^+ = U_B^*/u_\tau$. Since the u_τ -normalization is mainly used throughout this study, we will only show the explicit solution of system (B.9), which reads

$$\hat{U}_1^+(x'_2) = \frac{x'_2}{v_0^+} - \frac{2}{v_0^+} \frac{e^{v_0^+ Re_\tau x'_2} - 1}{e^{2v_0^+ Re_\tau} - 1}, \quad \text{with} \quad u_\tau = U_B^* v_0^+ \cdot \frac{v_0^+ Re_\tau}{v_0^+ Re_\tau \cdot \coth(v_0^+ Re_\tau) - 1}, \quad (\text{B.10})$$

or, in the non-normalized (dimensionalized) form, as:

$$\frac{U_1^L(x_2/h)}{u_\tau^L} = \frac{x_2/h}{v_0^+} - \frac{2}{v_0^+} \frac{e^{v_0^+ Re_\tau x_2/h} - 1}{e^{2v_0^+ Re_\tau} - 1}, \quad u_\tau^L = U_B^* v_0^+ \cdot \frac{v_0^+ Re_\tau}{v_0^+ Re_\tau \cdot \coth(v_0^+ Re_\tau) - 1}, \quad (\text{B.11})$$

where we used the notation $U_1 = U_1^L$ and $u_\tau = u_\tau^L$ from Section 3 & 4 to distinguish these quantities from the corresponding turbulent flow behavior. The initial (dimensionalized) system parameters v_0 , K and ν as given (B.3) are then related to the three independently chosen ones v_0^+ , Re_τ and U_B^* as follows:

$$\left. \begin{aligned} v_0 &= U_B^* v_0^{+2} \frac{v_0^+ Re_\tau}{v_0^+ Re_\tau \cdot \coth(v_0^+ Re_\tau) - 1}, & K &= \frac{U_B^{*2} v_0^{+2}}{h} \left(\frac{v_0^+ Re_\tau}{v_0^+ Re_\tau \cdot \coth(v_0^+ Re_\tau) - 1} \right)^2, \\ \nu &= \frac{U_B^* v_0^+ h}{Re_\tau} \frac{v_0^+ Re_\tau}{v_0^+ Re_\tau \cdot \coth(v_0^+ Re_\tau) - 1}. \end{aligned} \right\} \quad (\text{B.12})$$

Hence, note that when initializing in the u_τ -normalization the two independent system parameters v_0^+ and Re_τ , then the transpiration parameter normalized on the universal bulk velocity, i.e. v_0/U_B^* , is determined as

$$\frac{v_0}{U_B^*} = v_0^{+2} \frac{v_0^+ Re_\tau}{v_0^+ Re_\tau \cdot \coth(v_0^+ Re_\tau) - 1}, \quad (\text{B.13})$$

which converges to v_0^{+2} in the limit $Re_\tau \rightarrow \infty$ at a fixed transpiration rate v_0^+ . In other words, although the transpiration rate v_0^+ inside the u_τ -normalization can be chosen independently from Re_τ , it is not so for the bulk-velocity-normalized transpiration rate v_0/U_B^* , which is even bounded when the Reynolds number goes to infinity: $\lim_{Re_\tau \rightarrow \infty} v_0/U_B^* = v_0^{+2}$, a property also to be expected in the turbulent case, but where the value of course is unknown; see Table 4.

References

- AVSARKISOV, V. 2013 *Turbulent Poiseuille Flow with Uniform Wall Blowing and Suction*. PhD Thesis, TU Darmstadt.
- AVSARKISOV, V., OBERLACK, M. & HOYAS, S. 2014 New scaling laws for turbulent Poiseuille flow with wall transpiration. *J. Fluid Mech.* **746**, 99–122.
- CHANG, C.-Y. 2009 *Direct Numerical Simulation of Channel flow with Wall Transpiration*. Master Thesis, TU Darmstadt.
- FREWER, M. 2015a An example elucidating the mathematical situation in the statistical non-uniqueness problem of turbulence. [arXiv:1508.06962](https://arxiv.org/abs/1508.06962).
- FREWER, M. 2015b Application of Lie-group symmetry analysis to an infinite hierarchy of differential equations at the example of first order ODEs. [arXiv:1511.00002](https://arxiv.org/abs/1511.00002).
- FREWER, M. 2015c On a remark from John von Neumann applicable to the symmetry induced turbulent scaling laws generated by the new theory of Oberlack et al. [ResearchGate](https://www.researchgate.net/publication/311111111), doi:10.13140/RG.2.1.4631.9446, pp. 1–3.
- FREWER, M., KHUJADZE, G. & FOYSI, H. 2014 On the physical inconsistency of a new statistical scaling symmetry in incompressible Navier-Stokes turbulence. [arXiv:1412.3061](https://arxiv.org/abs/1412.3061).
- FREWER, M., KHUJADZE, G. & FOYSI, H. 2015 Comment on “Statistical symmetries of the Lundgren-Monin-Novikov hierarchy”. *Phys. Rev. E* **92**, 067001.
- FREWER, M., KHUJADZE, G. & FOYSI, H. 2016 A note on the notion “statistical symmetry”. [arXiv:1602.08039](https://arxiv.org/abs/1602.08039).
- KHUJADZE, G. & OBERLACK, M. 2004 DNS and scaling laws from new symmetries of ZPG turbulent boundary layer flow. *Theor. Comp. Fluid Dyn.* **18**, 391–411.
- OBERLACK, M. 2000 *Symmetrie, Invarianz und Selbstähnlichkeit in der Turbulenz*. Habilitation, Fakultät für Maschinenwesen, RWTH Aachen.
- OBERLACK, M. 2001 A unified approach for symmetries in plane parallel turbulent shear flows. *J. Fluid Mech.* **427**, 299–328.
- OBERLACK, M. 2002 Symmetries and invariant solutions of turbulent flows and their implications for turbulence modelling. In *Theories of Turbulence* (ed. M. Oberlack & F. H. Busse), pp. 301–366. Springer.

- OBERLACK, M. & GUENTHER, S. 2003 Shear-free turbulent diffusion - classical and new scaling laws. *Fluid Dyn. Res.* **33**, 453–476.
- OBERLACK, M. & ROSTECK, A. 2010 New statistical symmetries of the multi-point equations and its importance for turbulent scaling laws. *Discrete Continuous Dyn. Syst. Ser. S* **3**, 451–471.
- OBERLACK, M., WACŁAWCZYK, M., ROSTECK, A. & AVSARKISOV, V. 2015 Symmetries and their importance for statistical turbulence theory. *Mech. Eng. Rev.* **2** (2), 15–00157.
- ROSTECK, A. 2014 *Scaling Laws in Turbulence — A Theoretical Approach Using Lie-Point Symmetries*. PhD Thesis, TU Darmstadt.
- TENNEKES, H. & LUMLEY, J. L. 1972 *A First Course in Turbulence*. MIT Press.